



**Nuno Alexandre dos  
Santos Dias**

**A low-cost and low-power hole-detecting cane for  
the visually impaired**

**Bengala de apoio a cegos com detecção de buracos**





**Nuno Alexandre dos  
Santos Dias**

**A low cost and low-power hole-detecting cane for the  
visually impaired**

**Bengala de apoio a cegos com detecção de buracos**

Thesis submitted to Universidade de Aveiro [University of Aveiro] in partial fulfilment of the requirements for the degree of Master in Engenharia Electrónica e de Telecomunicações [Electronics and Telecommunications Engineering]. Thesis supervised by PhD José Manuel Neto Vieira, Professor Auxiliar of the Departamento de Electrónica, Telecomunicações e Informática of Universidade de Aveiro.

Dissertação apresentada à Universidade de Aveiro para cumprimento dos requisitos necessários à obtenção do grau de Mestre em Engenharia Electrónica e de Telecomunicações, realizada sob a orientação científica do Dr. José Manuel Neto Vieira, Professor Auxiliar do Departamento de Electrónica, Telecomunicações e Informática da Universidade de Aveiro.



I dedicate this work to all disabled persons, particularly the visually impaired.



**the jury**

chairman

**Doutor Alexandre Manuel Moutela Nunes da Mota**

Professor Associado from Universidade de Aveiro

**Doutor Diamantino Rui da Silva Freitas**

Professor Associado from Departamento de Engenharia Electrotécnica e de Computadores  
of Faculdade de Engenharia da Universidade do Porto

**Doutor José Manuel Neto Vieira**

Professor Auxiliar from Universidade de Aveiro

**Doutor João Manuel de Oliveira e Silva Rodrigues**

Professor Auxiliar from Universidade de Aveiro



## **Acknowledgements**

I wish to express my deep gratitude to Professor José Manuel Neto Vieira for giving me the opportunity to start this exciting project and, above all, for all the help, patience, guidance and words of wisdom. Throughout this year, I have learned a lot more than mere science.

I would also like to thank Professors Rui Manuel Escadas Ramos Martins and João Manuel de Oliveira e Silva Rodrigues for the fresh and innovative ideas as well as for all the help provided during the project.

Finally, a very special word of gratitude goes to all my family and friends, whose support, companionship and understanding I will never forget.



**keywords**

Mobility, visually impaired, obstacle detection, low-power, ultrasounds, cane.

**abstract**

This work proposes a new cane for the visually impaired which is capable of detecting holes, drop-offs and steps, designed with the main purpose of improving the mobility of visually impaired individuals. A small research was initially conducted and showed that currently available “intelligent” canes only provide detection of obstacles ahead of the subject, obstacles which would be easily detected by physical contact with any regular cane. Furthermore, in conversations with visually impaired associations, it became clear that holes, drop-offs and steps are among their greatest concerns, especially uncovered sewer manholes, helping to realize that this was one of the fields where technological research and development should be focused.

Throughout this work, there was a great concern in the low-power consumption of the device, as well as the overall low cost of a hypothetically final product. The developed techniques for hole-detection rely on pulses of ultrasounds. Solar power is used to keep the batteries charged so that the user does not need to worry about changing or charging any batteries on a regular basis. Another innovative feature of this cane is related with the increasing visibility and safety provided to the user under dark conditions, especially when crossing streets or in heavy traffic areas. The cane automatically detects the ambient light and decides to turn on or off an array of blinking LEDs along the body of the cane. This enables drivers to recognize the user earlier and better, in order to take the necessary precautions. The means of interaction between the cane and the user are vibration and/or audible signals. Field tests proved and validated the concept and algorithms presented, allowing holes, drop-offs and steps to be detected flawlessly, and with only a very limited number of false detections occurring in very irregular surfaces. Nonetheless, all the holes were detected in every kind of surface, proving this is an efficient way of bringing a clear path to the visually impaired.

This work covers all the details concerning the development of this new device, as well as the results of practical field tests.



**palavras-chave**

Mobilidade, invisuais, detecção de obstáculos, baixa potência, ultra-sons, bengala.

**resumo**

Este trabalho propõe uma nova bengala para cegos e amblíopes concebida com o principal objectivo de melhorar a mobilidade dos seus utilizadores através da detecção de buracos, desníveis e degraus. Uma breve pesquisa mostrou que os dispositivos “inteligentes” actualmente disponíveis apenas fornecem detecção de obstáculos à frente do utilizador. Obstáculos que podem ser facilmente detectados por contacto físico com uma vulgar bengala.

Por outro lado, as associações de cegos e amblíopes deixam claro que os buracos, desníveis e degraus estão entre as suas maiores preocupações, especialmente buracos de esgoto sem tampa, mostrando que este é um campo onde a investigação e desenvolvimento tecnológicos deverão incidir.

Existiu uma grande preocupação relativamente ao baixo consumo energético do dispositivo, bem como com o baixo custo global de um hipotético produto final. As técnicas desenvolvidas para a detecção de buracos baseiam-se em pulsos de ultra-sons. É utilizada energia solar para manter as pilhas carregadas de modo que o utilizador não necessite de preocupar-se frequentemente com a mudança ou carregamento das baterias. Outra característica inovadora desta bengala está relacionada com o aumento de visibilidade e segurança proporcionado ao utilizador em ambientes nocturnos ou escuros, especialmente ao atravessar ruas ou em áreas de tráfego intenso. A bengala detecta automaticamente a luz ambiente e decide ligar ou desligar uma matriz de LEDs intermitentes dispostos ao longo da bengala. Isto permite que os condutores reconheçam antecipadamente e com mais segurança o invisual e tomem as precauções necessárias. Para interacção da bengala com o utilizador são utilizados vibração e/ou sinais sonoros. Testes realizados em ambientes reais provaram a validade do conceito e dos algoritmos apresentados, permitindo detectar eficazmente buracos, desníveis e degraus, verificando-se apenas um número muito limitado de falsas detecções em superfícies muito irregulares. No entanto, todos os buracos foram detectados independentemente do tipo de superfície, mostrando que a abordagem efectuada permite melhorar a mobilidade e confiança dos cegos e amblíopes de uma forma eficaz.

Este trabalho cobre todos os detalhes relativos ao desenvolvimento deste novo dispositivo, bem como os resultados obtidos.



# Contents

Contents.....	15
List of figures.....	17
List of tables.....	19
List of acronyms.....	21
1 INTRODUCTION.....	23
1.1 Motivation.....	23
1.2 Objectives.....	23
1.3 Overview.....	23
2 Mobility aid devices for the visually impaired.....	25
2.1 Currently available devices (state of the art).....	27
2.1.1 UltraCane.....	27
2.1.2 K-Sonar.....	28
2.1.3 DOPECA.....	29
2.1.4 MiniGuide.....	30
2.1.5 LaserCane-2000.....	31
2.1.6 NavBelt and GuideCane.....	32
2.1.7 Wearable Obstacle Detection System.....	33
2.1.8 CyARM.....	34
2.1.9 Ultra Body Guard.....	35
2.1.10 Guido Smart Walker.....	36
2.1.11 Sonic Pathfinder.....	37
2.1.12 The vOICe.....	38
2.2 Our cane.....	40
2.2.1 Our specifications.....	40
3 Hole-detection techniques using ultrasounds.....	41
3.1 Measuring distances with ultrasounds.....	42
3.2 Identification of the factors that affect the ultrasound response.....	43
3.2.1 Setup used.....	43
3.2.2 Obtained results with the sensors perpendicular to the ground.....	45
3.2.3 Obtained results with the sensors tilted relative to the ground.....	53
3.2.4 Acoustical direct path.....	55

3.2.5	Use of 4.5 Vpp do drive the emitter .....	55
3.2.6	Variation of the pulse width .....	58
3.2.7	Conclusions – problems encountered.....	61
3.3	The multipath effect .....	62
3.3.1	Effects on the pulse detection.....	62
3.3.2	Using two sensors to create spatial diversity and mitigate the multipath problem .....	63
3.3.3	Pulse averaging to solve the multipath problem.....	64
3.4	Hole-detection algorithm.....	65
3.4.1	Concept .....	65
3.4.2	Description .....	66
4	Hole-detecting cane .....	71
4.1	Development of the cane.....	71
4.2	Module #1 – Ultrasound control and hole-detection.....	71
4.2.1	Global module description .....	72
4.2.2	Block-wise description.....	73
4.2.3	Software .....	75
4.2.4	Developed Hardware.....	76
4.3	Module #2 - Power, LEDs and feedback .....	77
4.3.1	Global module description .....	77
4.3.2	How the module works .....	78
4.3.3	Block-wise description.....	78
4.3.4	Software .....	81
4.3.5	Proposed prototype of module #2 .....	83
4.3.6	Results / Problems encountered .....	85
4.3.7	Conclusions .....	87
4.4	Proposed prototype of the cane – full system.....	87
5	Field tests / Results .....	89
6	Conclusions.....	91
7	Bibliography .....	93
Appendix A	Circuit schematics .....	95
Appendix B	PCBs.....	99
Appendix C	Software .....	101
Appendix D	Characterization of the noise present in the received echoes .....	103
Appendix E	Detection of sudden changes in the amplitude of the echoes.....	107

## List of figures

Figure 2-1: UltraCane .....	27
Figure 2-2: K-Sonar .....	28
Figure 2-3: MiniGuide .....	30
Figure 2-4: LaserCane-2000.....	31
Figure 2-5: NavBelt and GuideCane.....	32
Figure 2-6: Functional diagram of the GuideCane.....	33
Figure 2-7: Wearable Obstacle Detection System .....	34
Figure 2-8: CyARM.....	35
Figure 2-9: Ultra Body Guard .....	36
Figure 2-10: Guido Smart Walker.....	37
Figure 2-11: Sonic Pathfinder .....	38
Figure 2-12: The vOICe .....	39
Figure 3-1: Basic building block of distance measurement using ultrasounds .....	41
Figure 3-2: Wood structure holding the ultrasonic emitter and receiver.....	43
Figure 3-3: Emitter and receiver placed inside aluminum tubes.....	44
Figure 3-4: Signal used to drive the ultrasonic emitter - 12-cycle burst of 40-kHz sin-wave.....	44
Figure 3-5: Connection between the several elements .....	45
Figure 3-6: Direct path and response components (echo) of the received signal.....	45
Figure 3-7: Tested surface - Linoleum.....	46
Figure 3-8: Sent (CH1) and received (CH2) signals (amplitude and time) - Linoleum.....	46
Figure 3-9: Tested surface and received signal - Carpet.....	47
Figure 3-10: Tested surface - Tile .....	47
Figure 3-11: Received signal – Tile .....	48
Figure 3-12: Tested surface – Rubber #1 .....	48
Figure 3-13: Received signal – Rubber #1 .....	48
Figure 3-14: Tested surface - Stone .....	49
Figure 3-15: Received signal - Stone .....	49
Figure 3-16: Tested surface - Rubber #2.....	50
Figure 3-17: Received signal - Rubber #2.....	50
Figure 3-18: Tested surface and received signal - Irregular surface of rubber and metal .....	51
Figure 3-19: Tested surface and received signal - Portuguese paving .....	51
Figure 3-20: Tested surface and received signal - Tar .....	52
Figure 3-21: Response at 0 degrees.....	53
Figure 3-22: Used test setup and obtained response at 22.5 degrees .....	53
Figure 3-23: Used test setup and obtained response at 45 degrees .....	54
Figure 3-24: Used test setup and obtained response at 65 degrees .....	54
Figure 3-25: Received signal without and with a paper inserted .....	55
Figure 3-26: Driving signal with 4.5V .....	55
Figure 3-27: Response to the 4.5V signal - linoleum at 30cm.....	56
Figure 3-28: Response to the 4.5V signal - carpet at 30cm .....	56
Figure 3-29: Response to the 4.5V signal - linoleum at 10cm.....	57
Figure 3-30: Response to the 4.5V signal - linoleum at 50cm.....	57
Figure 3-31: Response to a 300 $\mu$ s burst.....	58
Figure 3-32: Response to a 450 $\mu$ s burst.....	58
Figure 3-33: Response to a 200 $\mu$ s burst.....	59

Figure 3-34: Response to a 150 $\mu$ s burst.....	59
Figure 3-35: Response to a 100 $\mu$ s burst.....	60
Figure 3-36: Response to a 50 $\mu$ s burst.....	60
Figure 3-37: Received pulses from Portuguese paving.....	63
Figure 3-38: Received pulses from grass .....	63
Figure 3-39: Placement of the sensors and example of multipath.....	64
Figure 3-40: Example of a sequence of pulses after processing .....	65
Figure 3-41: Conceptual flowchart of the hole-detection algorithm developed in Matlab .....	66
Figure 3-42: Received echo at the input channel of the microcontroller's ADC.....	67
Figure 3-43: Example of the method for calculating the slope of the distance variation.....	69
Figure 4-1: Block diagram of module #1 .....	72
Figure 4-2: eZ430-RF2500 Development Tool.....	73
Figure 4-3: Voltage regulation circuit (MAX1675).....	74
Figure 4-4: Module #1 .....	76
Figure 4-5: Module #1 - front and rear panel.....	76
Figure 4-6: Block diagram of module #2.....	77
Figure 4-7: LEDs driving circuit.....	80
Figure 4-8: eZ430-F2013 development tool .....	81
Figure 4-9: Flowchart of the module #2 microcontroller software .....	82
Figure 4-10: PCB with relevant components of module #2.....	84
Figure 4-11: Flexible solar panel placed around the prototype cane.....	84
Figure 4-12: High brightness LED and connectors.....	84
Figure 4-13: Full prototype version of module #2 .....	85
Figure 4-14: Using an LED as a voltage regulator.....	86
Figure 4-15: Modules' interconnection diagram .....	88
Figure 4-16: Prototype of the cane.....	88
Figure 5-1: Field tests with a blind person.....	89
Figure 7-1: Electrical schematic of module #2 .....	95
Figure 7-2: Electrical schematic of module #1 .....	96
Figure 7-3: Schematic of the external RS232 interface .....	97
Figure 7-4: PCB of module #2 (bottom and top views).....	99
Figure 7-5: PCB of module #1 (bottom and top views).....	99
Figure 7-6: PBC of the external RS232 interface (bottom and top views) .....	100
Figure 7-7: Sequence for blinking the safety LEDs .....	101
Figure 7-8: Example of blinking a pair of LEDs.....	101
Figure 7-9: Activation and use of the ADC to measure the voltage of the solar panel.....	102
Figure 7-10: Average noise of channel 0 and channel 1 – emitter on.....	103
Figure 7-11: Linear fitting equations for channels 0 and 1 – emitter on.....	103
Figure 7-12: Average noise of channel 0 and channel 1 – emitter off .....	103
Figure 7-13: Linear fitting equations for channels 0 and 1 – emitter off .....	104
Figure 7-14: Calculated threshold for channel 0.....	104
Figure 7-15: Calculated threshold for channel 1 .....	104
Figure 7-16: Thresholds comparison for channels 0 and 1 .....	105
Figure 7-17: Example of the amplitude's slope detection algorithm.....	107
Figure 7-18: Comparison between amplitude and distance detection algorithms when echoes stop being received during small instants .....	108
Figure 7-19: Performance of both hole-detection algorithms over a deep and narrow hole.....	109

## List of tables

Table 1: Characteristics' summary of presented devices .....	26
Table 2: Summary of the factors that affect the ultrasounds response.....	61



## List of acronyms

ADC	Analog to Digital Converter
APEC	Associação Promotora do Ensino dos Cegos (a Portuguese association for the promotion of the education of visually impaired persons)
DCO	Digitally Controlled Oscillator
IIR	Infinite Impulse Response
ISR	Interrupt Service Routine
LED	Light-Emitting Diode
LPM	Low-Power Mode
PC	Personal Computer
PCB	Printed Circuit Board
SPL	Sound Pressure Level
UART	Universal Asynchronous Receiver Transmitter
USB	Universal Serial Bus



# 1 INTRODUCTION

## *1.1 Motivation*

It is only possible, for most people, to have a remote idea of what really means to be blind. One of the major limitations will undoubtedly be the mobility of a visually impaired person. Thus, this is a matter that science and technology must try to mitigate.

In the specific case of mobility, there are, although in smaller numbers than desirable, several isolated cases of research and development in the area of electronic devices that seek to improve the mobility of visually impaired people. Even fewer are the devices that actually reach a stage of production and marketing, and those who do, usually have very high prices, representing an economical burden that may be unacceptable for most users.

The idea of creating this project appeared in meetings and conversations with APEC. They focused their actual major mobility issues: holes, especially open sewers lids, and low profile objects on the floor, which couldn't be detected by traditional canes, but were enough for a person to stumble and fall. They explained that most of the currently available "intelligent" devices, when compared to regular canes, only added the detection of somewhat large obstacles ahead of the user and/or were prohibitively expensive for the common user. In addition, it was clear that this kind of obstacles can already be easily detected by physical contact with any traditional cane. It was obvious, at this point, that there was something to be done.

## *1.2 Objectives*

This project was started with the main objectives of bringing hole-detection (and detection of small obstacles laying on the ground, to some extent) in a low cost device, which could be accessible to the widest possible range of visually impaired persons. The device should be physically similar to a traditional cane in order to look familiar to the user and provide feedback about holes using vibration. It should also provide visible signals to drivers during dark conditions, improving the user's safety when crossing streets during the night. The use of low-power electronics and algorithms was an important requirement and power consumption should be kept as low as possible, so that small batteries could be used, and in the smallest number possible. Due to the requirement of low cost, all the components of the device should be carefully selected to best fit the compromise between price, availability, quality and desired requirements.

## *1.3 Overview*

The work starts with a chapter introducing the currently available devices developed with the main objective of improving the mobility of the visually impaired. Chapter 3 will then focus on the techniques developed to detect holes using ultrasonic sensors. It will show preliminary tests that were conducted to study the behaviour of ultrasounds using different kinds of surfaces, focusing on the several problems that were encountered as well as on the respective techniques developed to answer these problems. The main algorithm developed for hole-detection is presented at the end of this chapter. Chapter 4 addresses the development of the cane itself, specifically the hardware, and is followed by chapter 5 that concerns the practical results and field tests. Global conclusions are given in chapter 6.



## **2 Mobility aid devices for the visually impaired**

The first stage of this project was to conduct a relatively thorough search in order to find what kind of devices designed to improve the mobility of the visually impaired were currently available on the market or under development, and identify which features haven't still been addressed by these devices, especially concerning hole detection. The main targets of this search were products based on ultrasonic technology, although some other products were included due to their interesting properties, like laser technology. This choice for ultrasonic technology comes mainly from cost related issues, availability, ease of implementation, and power consumption. Ultrasonic transducers present a good balance between these properties.

The results of this search are presented in the following section, and an effort has been done in order to present the most relevant information of each device in a clear and concise way, providing several web links that can be consulted to find detailed information. From the gathered information, a small list of the pros and cons of each device was also made. Of all the devices presented, only the UltraCane was tested in our laboratory.

Table 1 presents a global summary of the main characteristic of the devices that will be presented in the next section.

Device	Type	Main objective	Sensors	Feedback	Power source	Features	Holes detection	Price
UltraCane	Cane	Detection of obstacles	Ultrasounds	Vibration	2×AA batteries	Detection of obstacles on the floor and above the waist level.	No	900 Eur
K-Sonar	Handheld device that can be attached to a cane	Detection of obstacles	Ultrasounds	Audio	Rechargeable batteries	Allows the user to recognize different objects and textures.	No	700\$
DOPECA	Glove - complement to a regular cane	Detection of obstacles	Ultrasounds	Vibration	Unknown	Detects obstacles above the waist level.	No	Under development
MiniGuide	Handheld device - complement to a traditional cane	Detection of obstacles	Ultrasounds	Vibration and audio	Type 123 Lithium battery	Gap finding mode.	No	Unknown
LaserCane-2000	Cane	Detection of obstacles and drop-offs	Laser	Vibration and audio	2×AA batteries	Detects drop-offs and obstacles at head-height and straight-ahead.	Yes	3000\$
NavBelt and GuideCane	Wearable belt and wheeled cane respectively	Detection and avoidance of obstacles	Ultrasounds	Audio and mechanical	Unknown	Actively guides the user through a clear path (without obstacles).	No	Under development
Wearable Obstacle detection System	Wearable jacket	Detection of obstacles	Ultrasounds	Vibration	Unknown	Hands-free device. Informs the user about the direction of the obstacle.	No	Unknown
CyARM	Handheld device	Detection of obstacles	Ultrasounds	Mechanical	Unknown	Directly informs the user about the obstacle's distance.	No	Under development
Ultra Body Guard	Handheld or chest-mounted device	Detection of obstacles	Ultrasounds	Vibration and voice	Unknown	Light sensor for orientation to light sources.	No	Unknown
Guido Smart Walker	Guidance vehicle	Mobility aid, navigation and automatic obstacle avoidance	Ultrasounds, lasers and encoders on the wheels	Mechanical and audio	Unknown	Automatically avoids collision and provides a clear path to the user	Yes	Under development
Sonic Pathfinder	Headband	Detection of obstacles	Ultrasounds	Audio	Unknown	Hands-free device. Informs the user about the direction of the obstacle.	No	Unknown
The vOICE	Special sunglasses	Detection of obstacles and perception of the environment.	Video camera	Audio	Laptop's battery	Translates video into sound	No	Free software. Requires a laptop and a camera
Our cane	Cane	Detection of holes, steps and drop-offs	Ultrasounds	Vibration and audio	Solar energy and 2×AAA batteries	Actively signals the presence of the user under dark environments. Automatically recharges the batteries (under solar light).	Yes	Under development but very low-cost

**Table 1: Characteristics' summary of presented devices**

## 2.1 Currently available devices (state of the art)

### 2.1.1 UltraCane

- <http://www.soundforesight.co.uk>
- Developed by the company Sound Foresight, founded in 1998 by researchers at the University of Leeds.
- Available in Portugal through: Ataraxia - ESTI, Lda, R.Damiao de Góis no2-3 Esq., 2650-322 Amadora, Portugal, E-mail: [ataraxia@ataraxia.pt](mailto:ataraxia@ataraxia.pt)
- Simple detection of objects using pulses of ultrasounds.
- Alerts the user through vibration in his thumb.
- Has two ultrasonic sensors, one for obstacles on the floor and the other for obstacles above the waist level. The wrist has two buttons (one associated with each sensor) that vibrate when an object is detected, varying the intensity of vibration according to the distance of the obstacle.
- Weight of the grip case: 300 g
- Battery life: 3-4 weeks
- Works with two AA batteries.



Figure 2-1: UltraCane

#### Pros:

- Detection of obstacles on the floor and above the waist level.
- Ability to adapt to the customer's needs:
- It can be adapted to according to the height and style of the customer:
- Available in 10 standard lengths from 105 cm to 150cm, with 5cm intervals.
- It can also be custom sized with any desired length, keeping the price unchanged.
- Different tips are available:
  - Pencil
  - Rollerball
  - Large Rollerball

**Cons:**

- Weight.
- Does not detect holes.
- Gives no information about the type of object being detected.
- Price: 900€

### 2.1.2 K-Sonar

- <http://www.batforblind.co.nz>
- Developed by the company Bay Advanced Technologies (BAT).
- One of the companies with higher reputation and with an extensive background in this area, having developed the successful SonicGuide in 1965.
- Uses 2 ultrasonic sensors to perceive the environment ahead of the user and constantly gives him information through audio signals in the provided headphones.
- The sound varies according to the distance and type of the object.
- As it uses chirp signals, it makes it possible to detect and recognize multiple objects.
- Relies on the brain's neural processing capability to discriminate between different objects.
- Scanned objects normally produce multiple echoes, translated by the receiver into 'tone-complex' sounds, which users constantly listen to and must learn to recognize.
- Rechargeable batteries. Power adapter is supplied.



**Figure 2-2: K-Sonar**

**Pros:**

- May be used with or without a cane. No special cane needed.
- Frequency chirps are used (bandwidth of one octave) instead of simple pulse-echo object detection, allowing the user to recognize different objects and textures.
- The user may choose between short and long range detection through a dedicated button.
- A good quality users' guide is provided and helpful training materials are also available.

**Cons:**

- Does not detect holes, drop-offs or steps.
- The user must learn to identify the sound signatures created.
- The ability to detect obstacles is not incorporated in the device, and depends on the user.
- Requires high levels of concentration from the user.
- It may reduce the user's audible perception of his surroundings and of the environment.
- Recommendation to charge the battery every night. Low battery life.
- Price: 700\$

### 2.1.3 DOPECA

- <http://www.adi.pt/sectores%20de%20actividade/projectos/dopeca.htm>
- DOPECA – Detector de Obstáculos para Pessoas Cegas e Amblíopes / Obstacle Detector for the Visually Impaired
- Developed for Agência da Inovação / Portuguese Innovation Agency by Faculdade de Engenharia da Universidade do Porto / Faculty of Engineering of the University of Porto, ACAPO - Associação para Cegos e Amblíopes de Portugal / Portuguese association for the visually impaired, and A. J. Fonseca, Lda.
- Still under development.
- Intends to be a complement to a regular cane. Detects obstacles above the waist level (distinction between three height levels).
- The prototype consists of a small bag, which is carried on the shoulder or waist, and contains the electronic circuits. It then connects to a special glove designed to be used in the hand which holds the cane.
- This glove contains ultrasonic sensors on the back of the hand and three vibrating actuators in the palm of the hand. These three actuators enable the user to distinguish the height and vertical position of the obstacle (high, middle and low).
- The rate of vibration depends on the distance of the obstacle.
- Based on the DSP TMS320C54
- Informative video: [http://darwin.fccn.pt/ainovacao/SAUDE\\_STR/DOPECA.mov](http://darwin.fccn.pt/ainovacao/SAUDE_STR/DOPECA.mov)

**Pros:**

- Detection of obstacles at head level.
- The use of vibration (instead of audio signals in earphones) does not interfere with the user's ability to listen to the sounds of the environment. These sounds are very important to the user's mobility, safety and perception of his surroundings.
- Can be used with or without any regular cane.
- According to the developers, the cost should be relatively low.

**Cons:**

- It does not detect holes, drop-offs or steps.
- The user needs to carry the containing the electronic circuits on the shoulder or waist.
- During the summer or hot days or environments, wearing the glove may turn out to be very uncomfortable.

### 2.1.4 MiniGuide

- [http://www.gdp-research.com.au/minig\\_1.htm](http://www.gdp-research.com.au/minig_1.htm)
- Developed by Greg Phillips from GDP Research, South Australia.
- Designed only to serve as complement to a traditional cane or a guide dog.
- Uses ultrasounds to detect obstacles and alerts the user through vibration or audio signals via headphones.
- A single multifunctional button allows to turn the device on or off and to switch between the following operation modes (obstacle detection ranges):
  - 4 meters;
  - 2 meters;
  - 1 meter;
  - Half meter;
  - 8 meters.

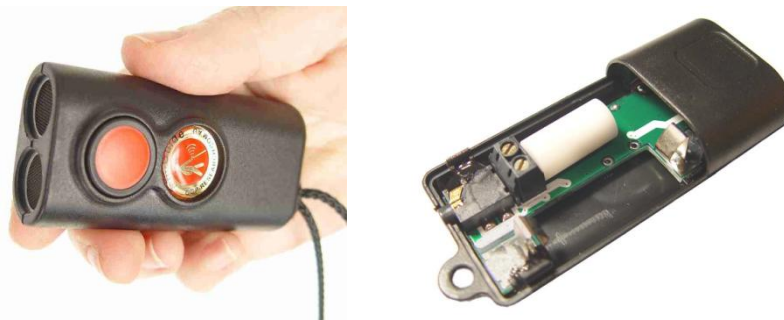


**Figure 2-3: MiniGuide**

**Pros:**

- The speed of vibration changes according to the distance of the obstacle.
- Offers the ability to optionally connect headphones for audible feedback..
- Gap finding mode to look for doors, entrances, windows, etc.
- Good battery life (one Type 123 Lithium battery) – according to the developer it should last for several months.
- May be pointed towards any direction, making it possible to detect obstacles at any height.
- Small and light – highly portable.

**Cons:**

- No holes, drop-offs or steps detection.
- If used with a cane or guide dog, leaves the user without any free hand.
- Non rechargeable battery.

### 2.1.5 LaserCane-2000

- [http://www.pco.edu/grad/om/om\\_photo/gs\\_om\\_photos\\_lasercane.htm](http://www.pco.edu/grad/om/om_photo/gs_om_photos_lasercane.htm)
- <http://www.photonics.com/content/spectra/2003/June/applications/65753.aspx>
- <http://www.eyeofthepacific.org/electronic%20aids.htm>
- [http://www.maxiaids.com/store/prodView.asp?idproduct=6247&idstore=1&idCategory=21&category=Canes&product=LaserCane\\_-\\_Custom](http://www.maxiaids.com/store/prodView.asp?idproduct=6247&idstore=1&idCategory=21&category=Canes&product=LaserCane_-_Custom)
- Developed by Nurion-Raycal, 2004.
- Under development since the 1970s.
- Employs diode lasers directed upward, forward and downward, and gated detectors monitor the returning light.
- Reflected light from the upward or forward channels indicates an obstacle. The absence of reflected light from the downward channel indicates a drop-off.
- Communicates with the user by emitting audible signals that indicate which detectors are receiving a return signal or by producing vibrations on the side of the cane that are felt with a finger.
- Powered by two AA size batteries.

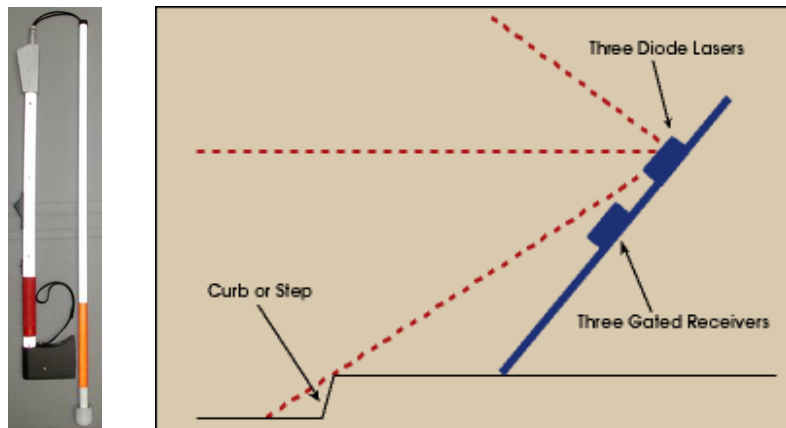


**Figure 2-4: LaserCane-2000**

**Pros:**

- Detects obstacles in the travel path at three levels - head-height, straight-ahead, and drop-offs.
- The user has the option of turning the audible tones off and rely only on vibrating stimulators.

**Cons:**

- Price: 3000\$
- Can only be folded in two sections.

### 2.1.6 NavBelt and GuideCane

- Developed by the University of Michigan's Mobile Robotics Lab
  - <http://ieeexplore.ieee.org/Xplore/login.jsp?url=/iel5/100/26709/01191706.pdf?arnumber=1191706>
  - <http://ieeexplore.ieee.org/iel5/100/26709/01191706.pdf?tp=&isnumber=26709&arnumber=1191706>
  - <http://www-personal.umich.edu/~johannb/Papers/chapter01.pdf>
  - [http://www-personal.umich.edu/~johannb/GC\\_News/GC\\_News.html](http://www-personal.umich.edu/~johannb/GC_News/GC_News.html)
- 
- NavBelt consists of a belt filled with ultrasonic sensors, intended to be used at the waist of the user.
  - Communicates with the user through stereo headphones, guiding him through the obstacles and providing an acoustic virtual image of his surroundings.
  - One of the limitations of the NavBelt is that it becomes very difficult and takes too much time for the user to decode and understand all the guidance signals provided, making it hard to keep a fast progress.
- 
- A newer device, GuideCane, solves this last problem. The GuideCane uses the same technology of NavBelt but instead of being used at the waist, is coupled to a device with wheels that is pushed through a walking stick.
  - When the GuideCane detects an obstacle, it turns away from it applying brakes on one or both wheels. The user immediately realizes the change of direction and simply follows the new route without having to think about it and without any effort.
  - Basically consists of a guidance system used in autonomous robots adapted for use with the visually impaired.
  - The GuideCane works almost like a guide dog. The user indicates the direction of the desired path through a mini joystick in the grip of the cane, and it follows that direction avoiding any obstacles.



Figure 2-5: NavBelt and GuideCane

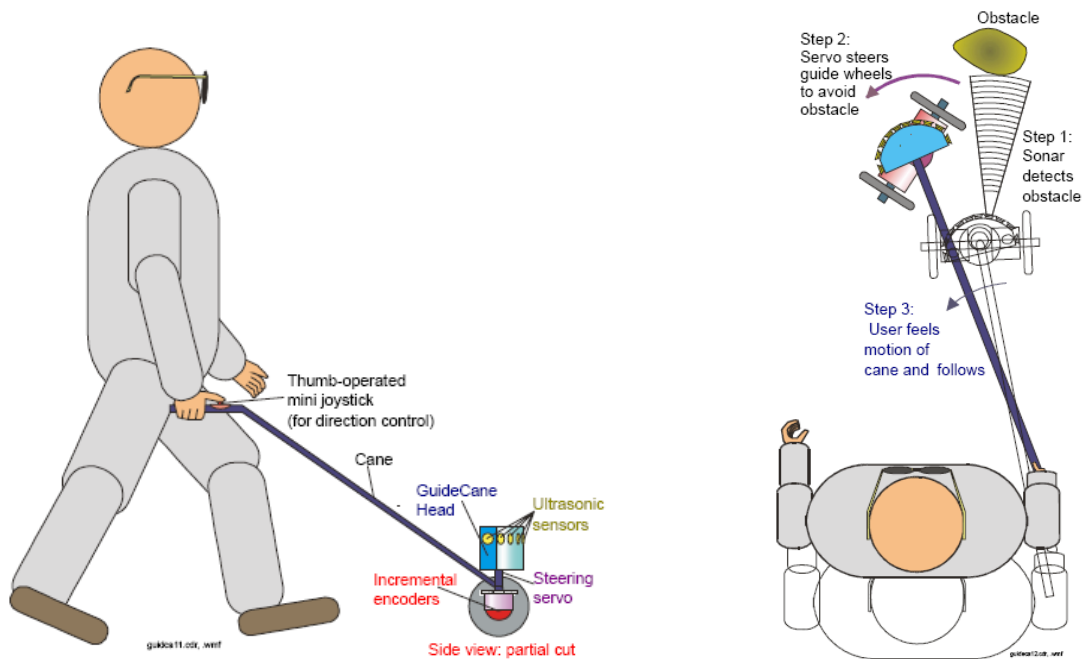


Figure 2-6: Functional diagram of the GuideCane

**Pros:**

- Wide range of features.
- The GuideCane frees the user of tasks such as moving a cane, decode the audio or tactile signals, and make the subsequent decisions. The user simply needs to follow the GuideCane.

**Cons:**

- Size.
- Weight (4Kg).
- Appearance (does not allow a discreet use).
- Does not detect holes or steps actively, although the user will feel them because the GuideCane would simply fall on a hole.
- Still under development - Commercially unavailable.

### 2.1.7 Wearable Obstacle Detection System

- Developed by the Virtual Reality Laboratory (VRlab) from Ecole Polytechnique Fédérale de Lausanne (EPFL)
- [http://vrlab.epfl.ch/Publications/pdf/Cardin\\_Vexo\\_Thalmann\\_Haptex\\_05.pdf](http://vrlab.epfl.ch/Publications/pdf/Cardin_Vexo_Thalmann_Haptex_05.pdf)
- Detects the closest obstacle through a stereo ultrasonic system and informs the user about the obstacle position using vibrators.
- The whole system is set in a jacket (or similar) designed to be worn by the user.
- The ultrasonic sensors and vibration units are placed on the shoulders of the user (an ultrasound transmitter/receiver pair on each shoulder).

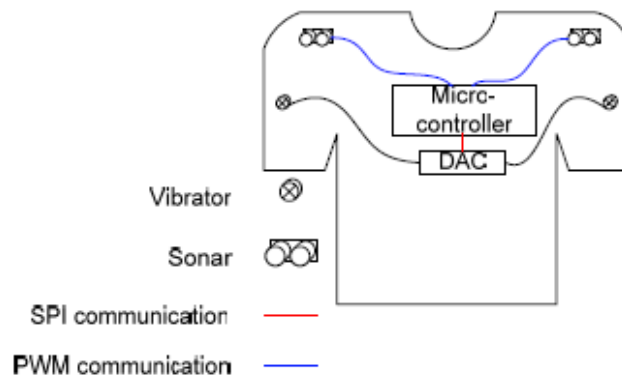


**Figure 2-7: Wearable Obstacle Detection System**

**Pros:**

- It's a hands-free device. The user keeps his hands free to use a traditional cane, guide dog, or any other device.
- Informs the user about the direction of the obstacle.
- Detects obstacles at head level.

**Cons:**

- The user will always be wearing the same piece of clothing.
- Doesn't detect holes or steps.
- Ineffective detection of small obstacles on the floor.
- Difficulties in the detection of doors, windows, etc.. Because if the user is in front of a door both sensors will detect the two side walls and thus inform the presence of an obstacle.
- Still under development - Commercially unavailable.

### 2.1.8 CyARM

- Developed in Japan by Future University-Hakodate, Kanazawa University, Ochanomizu University and Fuji Xerox Co. Ltd.
- <http://delivery.acm.org/10.1145/1060000/1056947/p1483-ito.pdf?key1=1056947&key2=1965059811&coll=GUIDE&dl=GUIDE&CFID=34685530&CFTOKEN=39402124>
- Measures the distance between the user and an object using ultrasonic sensors and informs the user about the distance through a movement on his arm.
- The CyARM connects to the user's waist through a wire. It then adjusts the tension of that wire according to the distance of the obstacle.
- When an object is close, the CyARM firmly pulls the wire so that the user's arm will move backwards. When this happens, the user knows that the object is within his reach. If the object is far away, CyARM releases the wire indicating that the object is not within his reach.



**Figure 2-8: CyARM**

**Pros:**

- The user doesn't need to make calculations, inferences or other high-level cognitive processes to determine the distance of a particular object and if whether or not it is in motion.
- The tension in the wire not only allows to detect distances, but also directions.
- It can thus be used either by children, the elderly or people with cognitive disabilities.

**Cons:**

- Does not detect holes, drop-offs and steps.
- Is still a prototype under development.

### ***2.1.9 Ultra Body Guard***

- Developed by RTB GmbH & Co. KG
- <http://www.rtb-bl.de/en/produkte/ubg.php>
- Supplement to a traditional white cane.
- Detection of obstacles using ultrasounds.
- Range to 1.90 m or 3 m.
- Light sensor for orientation to light sources.
- Communication with the user through vibration or voice.
- 2 languages are possible (German and English).
- Pedometer with Memo-Function.
- Obstacle perception with search function
- Compass and direction control



**Figure 2-9: Ultra Body Guard**

**Pros:**

- Double function as a chest-mounted system or as a handheld device.

**Cons:**

- Doesn't detect holes, drop-offs and steps.
- Lack of reliable information about the product.

### **2.1.10 Guido Smart Walker**

- Developed by Haptica Ltd.
- <http://www.haptica.com/id2.htm> <http://www.haptica.com/id4.htm>
- [http://www.disam.upm.es/~drodri/articles/RodriguezLosada\\_drt4all05.pdf](http://www.disam.upm.es/~drodri/articles/RodriguezLosada_drt4all05.pdf)
- Works both as a physical medium that provides support to the user and as a navigation and mobility aid device.
- Provides navigation and automatic collision avoidance for people with impaired vision and low mobility.
- Several technologies are implemented in Guido: Simultaneous Localization and Map Building (SLAM), pose tracking, path planning, collision avoidance and human robot interaction.
- Uses sensors to build a picture of its immediate environment: it identifies obstacles and openings and communicates these to the user via voice messages and through the steering.
- Automatically guides the user away from obstacles.
- Uses a laser range finder to detect obstacles straight ahead and ultrasonic sensors that work together with the laser (for redundancy) and are also used to identify obstacles on the sides and above Guido.
- Encoders monitor the wheels and provide information about the position of Guido.

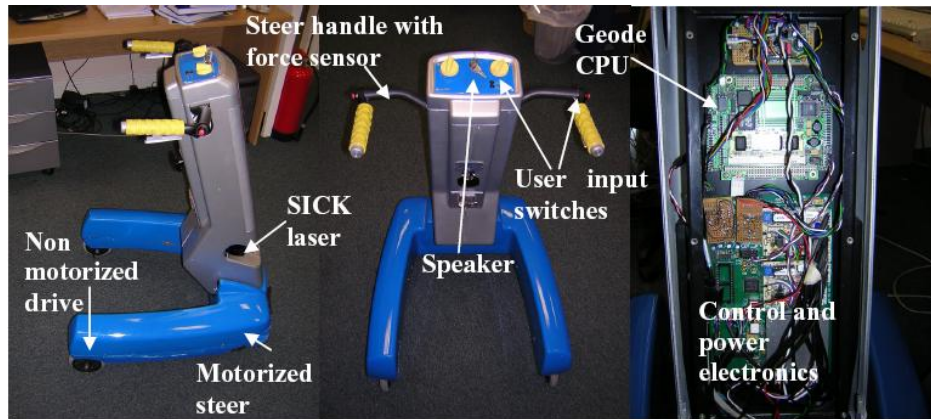


**Figure 2-10: Guido Smart Walker**

**Pros:**

- May be used by people with impaired vision or simply with low mobility.
- Automatically avoids collision and provides a clear path to the user without the need for his intervention.
- Uses a combination of different types of sensors (laser and ultrasonic) with some degree of redundancy.

**Cons:**

- Size and weight – not a portable device.
- Can hardly be used outdoors. Impossible to access public transports.
- Designed mainly for indoors (hospitals, homes and other buildings).
- It is not clear if it detects holes actively.
- Still under development.

### **2.1.11 Sonic Pathfinder**

- Developed by Perceptual Alternatives, Australia
- <http://www.abledata.com/abledata.cfm?pageid=19327&top=10267&productid=74626&trail=0&discontinued=0>
- [http://web.aanet.com.au/tonyheyes/pa/pf\\_blerb.html](http://web.aanet.com.au/tonyheyes/pa/pf_blerb.html)
- <http://www.sonicpathfinder.org/>

- To be used as a complement to a regular cane or guide dog.
- Consists in a headband that contains five ultrasonic sensors (2 emitters and 3 receivers) to be used in the forehead of the user.
- Informs the user about the direction of the obstacle through audible signals via stereo headphones.



**Figure 2-11: Sonic Pathfinder**

**Pros:**

- Detects and informs the direction of obstacles.
- Keeps the hands of the user free.

**Cons:**

- Not a discreet device. Might be uncomfortable to wear.
- Doesn't detect holes, drop-offs and steps.
- Identifies only one object at a time, giving priority to the closest object and the ones in front of the user.

### **2.1.12      *The vOICe***

- <http://www.seeingwithsound.com/>
- <http://www.seeingwithsound.com/winvoice.htm>
- Translates video images from a any regular camera (or webcam) into sounds, giving the user an audible image of his surroundings.
- Consists in a small camera, integrated in a pair of sunglasses. This camera then connects to a laptop computer which can be carried in a backpack. The computer translates the images into sound and sends the audible signal to the user through the headphones jack.
- Meant to be used as a supplement to a regular cane.



**Figure 2-12: The vOICe**

- Video is sounded in a left to right scanning order, by default at a rate of one image snapshot per second. The user hears the stereo sound pan from left to right correspondingly. Hearing some sound on the left or right means having a corresponding visual pattern on the left or right side of the user, respectively.
- During every scan, pitch means elevation: the higher the pitch, the higher the position of the visual pattern.
- Loudness means brightness: the louder the brighter. Consequently, silence means black, and a loud sound means white, and anything in between is a shade of grey.

**Pros:**

- The software is available free of charge, the user only needs to arrange the necessary hardware.
- Interesting technology with a good potential for satisfactory results, but it requires intensive training.
- Relatively discreet.

**Cons:**

- The sound produced is very stressful and does not allow the proper hearing from the surrounding environment.
- The user needs to carry a backpack with a laptop computer. Heavy and tiresome.
- Portability / Low battery life (laptop).
- Does not detect holes actively.

## ***2.2 Our cane***

It is evident the absence of a light, portable, discreet and effective device able to detect holes, drop-offs and steps. The detection of small objects on the ground that although not too large, are enough for someone to stumble and fall is also quite scarce. Also notorious is the very high price of most devices.

It is also important to notice that the vast majority of these devices took a considerably large period to develop (years) and that many of them are still prototypes under development and test.

Based on the evaluation of the devices presented earlier, our cane tries to mitigate some of the problems found on such devices and specifically brings hole-detection in a cheap, efficient and easy to use device.

### ***2.2.1 Our specifications***

The cane developed meets the following requirements:

- Use of ultrasounds to detect the floor.
- Detection of holes, drop-offs and steps.
- Detection of moderately low profile objects on the floor.
- Communication with the user through vibration and (optionally) audio signals.
- Detect dark environments in which it signals the presence of a visually impaired person by flashing high-brightness LEDs. Makes the user visible to drivers during the night.
- Very low power consumption for greater than average battery life.
- Built-in technique to recharge the batteries without requiring the intervention of the user.
- Use of clean renewable energy – solar power.
- Low-cost.
- Easy to use.
- Lightweight.
- Similar to a traditional cane, but with the electronic circuits incorporated.
- Can be used as a regular cane.

### 3 Hole-detection techniques using ultrasounds

A common, low-cost, straightforward and effective way to measure distances is to use ultrasonic sensors controlled by a microcontroller. Pulses of ultrasound are emitted followed by a listening period, in which the microcontroller tries to listen for echoes of the emitted pulse. These echoes appear when there is an object in the path of the emitted pulse.

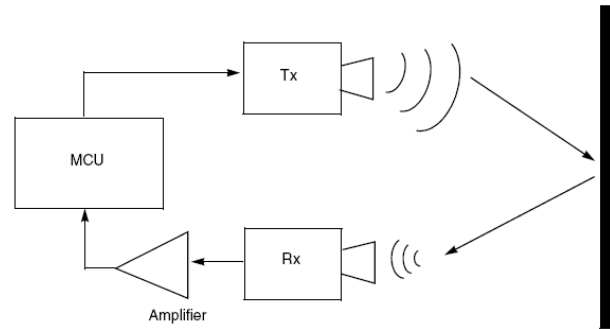


**Figure 3-1: Basic building block of distance measurement using ultrasounds**

A microcontroller (also  $\mu\text{C}$  or MCU) is a computer-on-a-chip, containing a processor, memory, and input/output functions. It is a microprocessor emphasizing high integration, in contrast to a general-purpose microprocessor (the kind used in a PC). In addition to the usual arithmetic and logic elements of a general purpose microprocessor, the microcontroller integrates additional elements such as read-write memory for data storage, read-only memory for program storage, EEPROM for permanent data storage, peripheral devices, and input/output interfaces. At clock speeds of as little as a few MHz or even lower, microcontrollers often operate at very low speed compared to modern day microprocessors, but this is adequate for typical applications. They consume relatively little power (milliwatts), and will generally have the ability to sleep while waiting for an interesting peripheral event such as a button press to wake them up again to do something. Power consumption while sleeping may be just nanowatts, making them ideal for low power and long lasting battery applications.

Ultrasound is cyclic sound pressure with a frequency greater than the upper limit of human hearing. Although this limit varies from person to person, it is approximately 20 kilohertz (20,000 hertz) in healthy, young adults and thus, 20 kHz serves as a useful lower limit in describing ultrasound. The ultrasound frequency used in this project is 40 kilohertz.

The basic concept used to detect holes, drop-offs and steps is to continually measure the distance from the cane to the ground. Of course in practice this is not so straightforward as it may look. One must take into account that the cane itself is constantly moving, thus changing its height relatively to the floor. Even more important and problematic than this, is the fact that the user can be walking on many different kinds of surfaces, like wood, tar, cement, linoleum, rubber, grass, dirt, stone, tiles, carpets, etc., or even a mixture between different elements and textures. Each kind of these surfaces presents a singular behaviour in response to the ultrasound pulses, making it very hard to obtain accurate measurements and sometimes even not responding to the ultrasound pulses at all. In addition to this, the cane can be used indoors as well as outdoors, increasing the type of environments where it must operate correctly.

Another difficulty to overcome is related to the use of low voltages and currents, being able to produce only weak pulses of ultrasounds, with small amplitudes, making the detection even harder and less immune to noise.

The following sections address the particularities of using ultrasounds to measure the distance to the floor.

### ***3.1 Measuring distances with ultrasounds***

The technique used to measure distances is similar to the echolocation used by bats, whales and dolphins, as well as SONAR used by submarines and boats. Echolocation is used by certain animals to locate food or obstacles in darkness, such as in caves and in the ocean. These animals produce sounds and then listen to the echoes. The delay between the emission of a sound and the arrival of an echo indicates the distance of an object.

The measurement of distances is based upon the reflection of sound waves. Sound waves are defined as longitudinal pressure waves in the medium in which they are travelling. Subjects whose dimensions are larger than the wavelength of the impinging sound waves reflect them; the reflected waves are called the echo. If the speed of sound in the medium is known and the time taken for the sound waves to travel the distance from the source to the subject and back to the source is measured, the distance from the source to the subject can be computed accurately. This is the basic principle of ultrasonic distance measurement. Here the medium for the sound waves is air, and the sound waves used are ultrasonic, since it is inaudible to humans.

Among others, ultrasounds offer the following advantages:

- Can be directed as a beam.
- Obey the laws of reflection and refraction.
- Are reflected by objects of small size (above the wavelength of the signal).

The speed at which sound travels depends on the medium which it passes through. In general, the speed of sound is proportional (the square root of the ratio) to the stiffness of the medium and its density. This is a fundamental property of the medium. In the air, speed of sound is approximately 344 m/s, in water 1500 m/s and in a bar of steel 5000 m/s. The speed of sound also changes with the conditions in the environment. For example, the speed of sound in the air depends on the temperature. Nominally, it is 344m/s at 25 degrees, dropping to 334m/s at 0 degrees.

The medium through which the sound travels in the following is always assumed to be air. Any material different from air is referred to as the object (this includes solids and liquids). All objects reflect, absorb and feed a portion of the wave through. The amplitude of the wave reflected is directly proportional to how much surface is available on the object for coherent reflection. Surface size, shape and orientation, are major factors contributing to the strength of the reflected signal; material composition is also a factor.

The precision in the measurement of the distance is not a relevant issue for this work. Thus, changes in temperature as well as other variations in the physical properties of sound propagation in air can and will be ignored.

Assuming that the speed of sound in air is 344 meters/second at room temperature and that the measured time taken for the sound waves to travel the distance from the source to the subject and back to the source is  $t$  seconds, the distance  $d$  is computed by the formula  $Distance = speed \times time \equiv d = 344 \times t$  meters. Since the sound waves travel twice the distance between the source and the subject, the actual distance between the source and the subject will be  $d/2$ .

## ***3.2 Identification of the factors that affect the ultrasound response***

The following practical tests intend to evaluate the behaviour of the ultrasounds when sending and receiving pulses from different floor surfaces and with variations of several factors, like distance, angle to the floor, driving voltage and pulse width. The chosen ultrasonic transducers are the Murata MA40S5 because they gather the desired requirements for this project and are very cheap. These tests were developed having in mind the particular characteristics needed for the possible implementation in the cane, like measurable distance, types of surfaces and supply voltages.

### ***3.2.1 Setup used***

Although the used transducers work as transceivers, it was decided to use two of these sensors separately, one working solely as an emitter and the other as a receiver, in order to improve their behaviour in an independent fashion.

Each transceiver was placed inside an aluminium tube of approximately the same diameter to ensure a snug fit. The use of the conductive tube around the sensor improves the electromagnetic shielding in order to better block noise and interferences. Both tubes were then placed together, forming the emitter-receiver pair, and positioned in a wooden support which allowed to set different heights in a relatively stable and precise fashion, thus guaranteeing the necessary repeatability to the experiments.

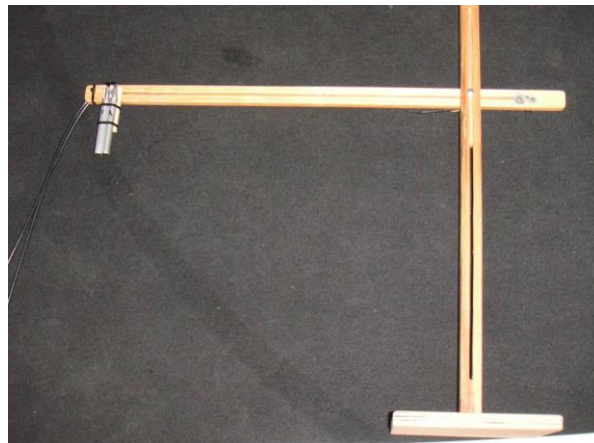


**Figure 3-2: Wood structure holding the ultrasonic emitter and receiver**

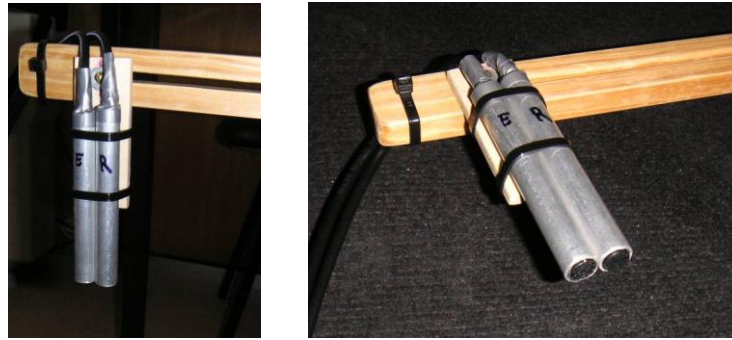


**Figure 3-3: Emitter and receiver placed inside aluminum tubes**

Without the use of any electronic circuits like gain amplifiers or filters, the receiver was directly connected to an oscilloscope and the emitter was directly connected to a function generator (for the  $40\text{ kHz}$  sinusoidal wave) which was in turn interconnected with a pulse generator (to control the duration of each pulse, and trigger the function generator). Basically, the pulse generator outputs the desired pulse that will modulate the  $40\text{ kHz}$  sinusoidal wave created by the function generator. The generated signal meant to drive the transmitter transducer consists of bursts with the duration of  $300\mu\text{s}$ , which corresponds to 12 periods of a  $40\text{ kHz}$  wave ( $12 \times 25\mu\text{s}$ ). The bursts were sent with a rate of  $50\text{ Hz}$ .

The obtained pulse (one burst) is depicted in the following picture:

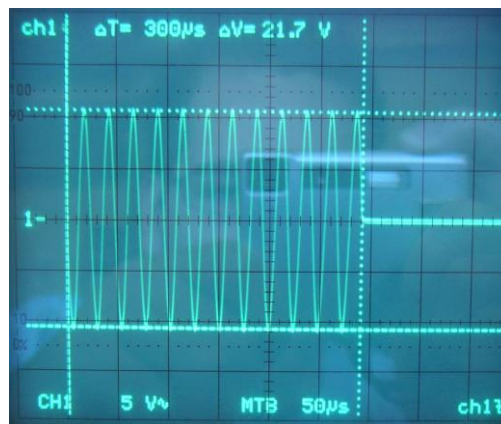


**Figure 3-4: Signal used to drive the ultrasonic emitter - 12-cycle burst of 40-kHz sin-wave**

The following photographs show the used setup with all the interconnections needed.



Figure 3-5: Connection between the several elements

### 3.2.2 Obtained results with the sensors perpendicular to the ground

The following measures were taken using the previously described 12-cycle 50 Hz bursts of 40-kHz sinusoidal-wave driving the emitter with peak-to-peak amplitude of approximately 20V. Unless stated cases, the height of the ultrasonic sensors was always kept between 10cm and 11cm. The emitter was connected to channel 1 of the oscilloscope and the receiver to channel 2. As it will be clearly visible in the following pictures, this setup produces a direct path between the emitter and the receiver (similar to crosstalk) causing a signal to appear in the response when the emitter sends ultrasonic pulses. This acoustical path is predominantly created through the air, between both sensors, but also has a small component that travels through the material. Nevertheless, this phenomenon is always constant and does not interfere with the desired measures. In addition, as it will be shown, this interference can be easily reduced.



Figure 3-6: Direct path and response components (echo) of the received signal

### 3.2.2.1 Linoleum



Figure 3-7: Tested surface - Linoleum

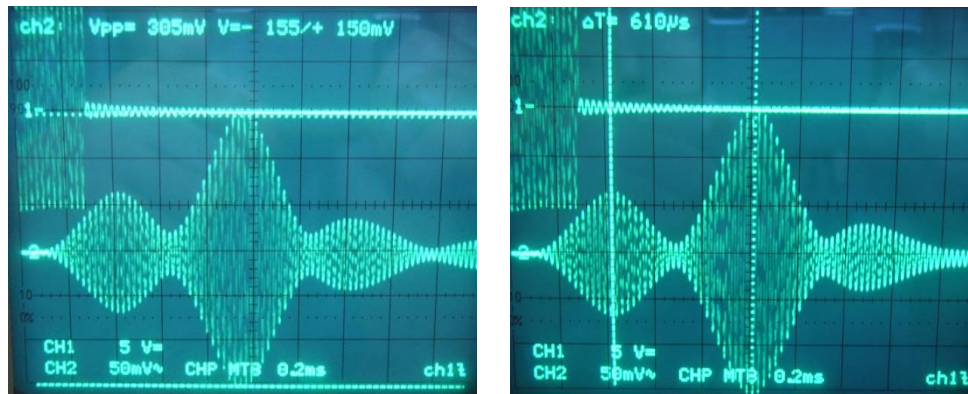


Figure 3-8: Sent (CH1) and received (CH2) signals (amplitude and time) - Linoleum

- Amplitude of the first echo:  $V_{pp} \cong 305mV$
- “Crosstalk”:  $V_{pp} \cong 136mV$  (always the same value)
- Time between the first two peaks (“crosstalk” and first echo):

$$\Delta t \cong 610\mu s \rightarrow d = \Delta t \times \frac{344m/s}{2} = 10,49cm$$

### 3.2.2.2 Carpet

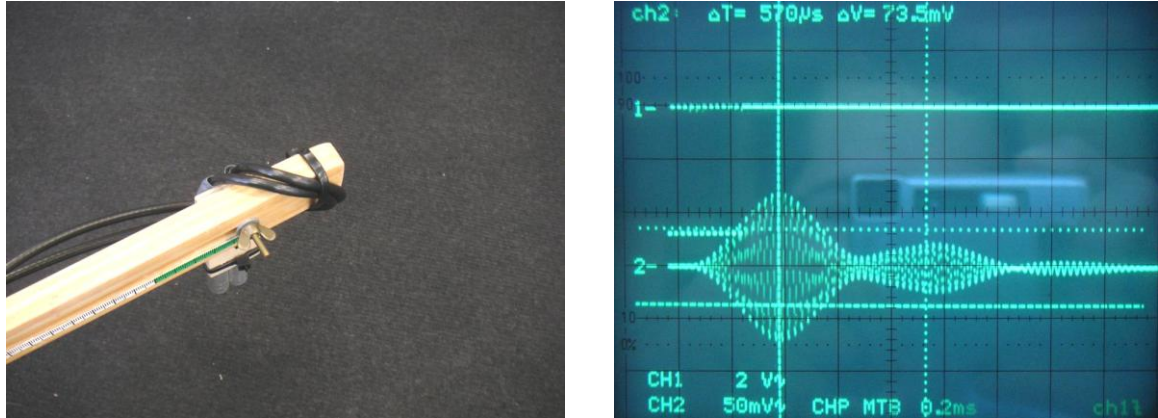


Figure 3-9: Tested surface and received signal - Carpet

- Amplitude of the first echo:  $V_{pp} \cong 70mV$
- Time between the first two peaks (“crosstalk” and first echo) of the response:  $\Delta t \cong 570\mu s$

It is evident the high attenuation experienced when detecting carpet. Nevertheless, and at least for these kind of short distances, the values are still acceptable.

### 3.2.2.3 Tile



Figure 3-10: Tested surface - Tile



Figure 3-11: Received signal – Tile

- Amplitude of the first echo:  $V_{pp} \cong 330mV$
- Time between the first two peaks (“crosstalk” and first echo) of the response:  $\Delta t \cong 568\mu s$

### 3.2.2.4 Rubber #1



Figure 3-12: Tested surface – Rubber #1

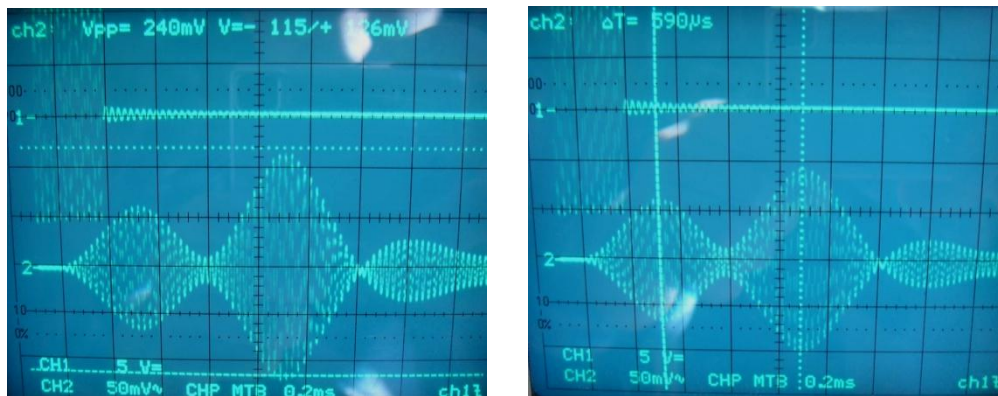


Figure 3-13: Received signal – Rubber #1

- Amplitude of the first echo:  $V_{pp} \cong 240mV$
- Time between the first two peaks (“crosstalk” and first echo) of the response:  $\Delta t \cong 590\mu s$

### 3.2.2.5 Stone



Figure 3-14: Tested surface - Stone

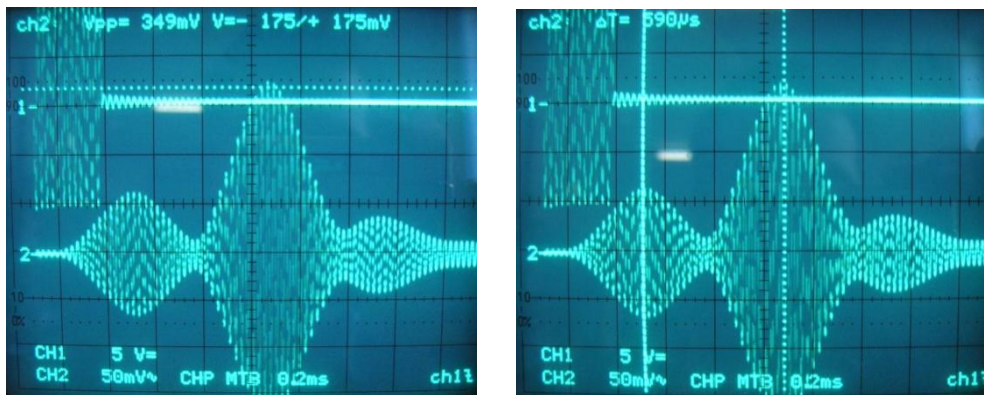


Figure 3-15: Received signal - Stone

- Amplitude of the first echo:  $V_{pp} \cong 349mV$
- Time between the first two peaks (“crosstalk” and first echo) of the response:  $\Delta t \cong 590\mu s$

### 3.2.2.6 Rubber #2



Figure 3-16: Tested surface - Rubber #2

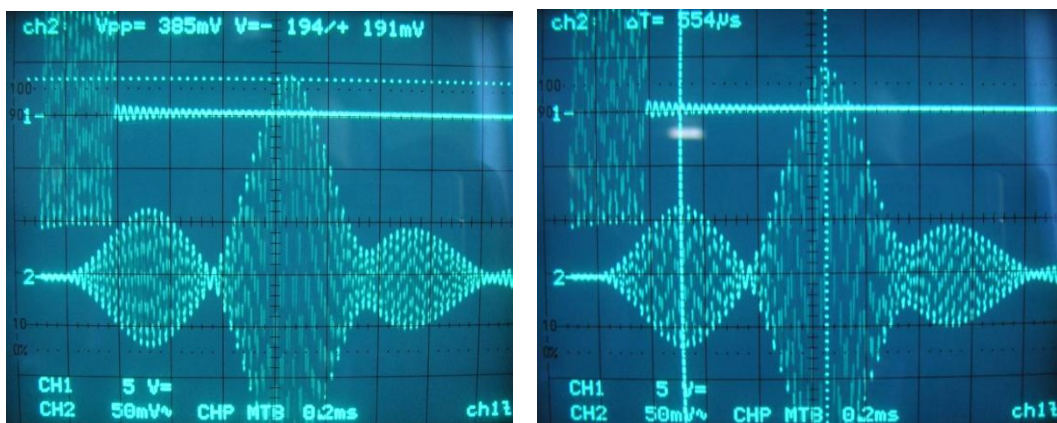


Figure 3-17: Received signal - Rubber #2

- Amplitude of the first echo:  $V_{pp} \cong 385mV$
- Time between the first two peaks (“crosstalk” and first echo) of the response:  $\Delta t \cong 554\mu s$

### 3.2.2.7 Irregular surface of rubber and metal - 11~14cm

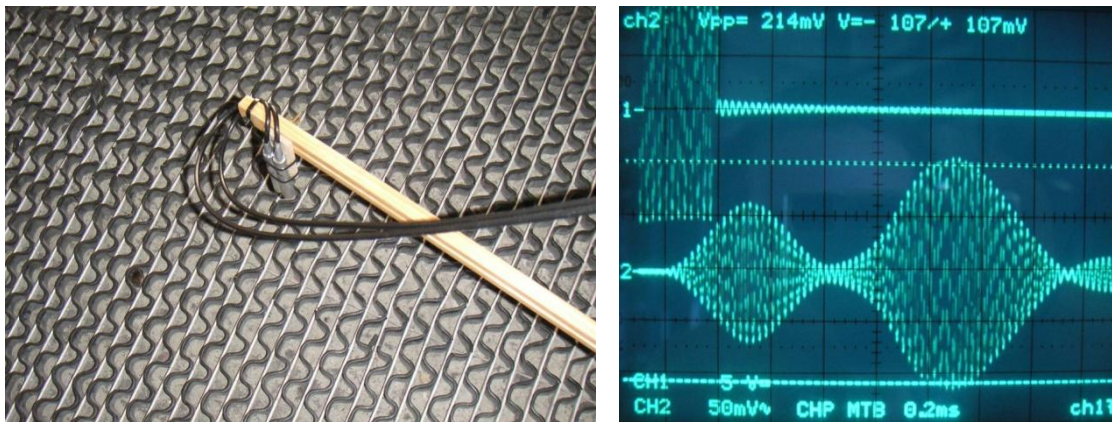


Figure 3-18: Tested surface and received signal - Irregular surface of rubber and metal

- Amplitude of the first echo:  $V_{pp} \cong 214mV$
- Time between the first two peaks (“crosstalk” and first echo) of the response:  $\Delta t \cong 740\mu s$

It is very important to notice the fact that the first echo is considerably wider in time than the ones from the previous surfaces. This is due to the multipath effect. More about this subject will be addressed in a following section.

### 3.2.2.8 Portuguese paving - 20cm

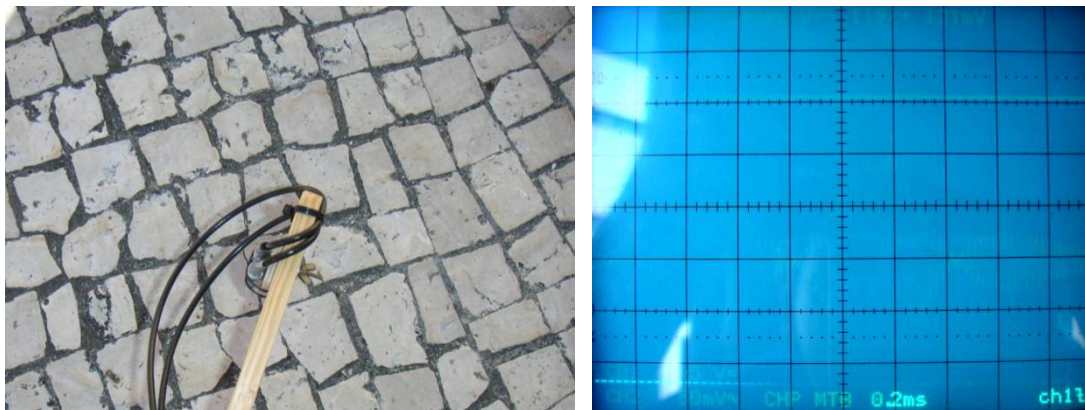


Figure 3-19: Tested surface and received signal - Portuguese paving

Unfortunately, due to the high intensity of the solar light, it was not possible to obtain pictures with acceptable quality.

This surface presented the worst and more problematical results off all the tested surfaces. It is very irregular surface and so it is the response to the pulses of ultrasounds. In many positions, the

amplitude of the received pulse is almost zero. This is due to the multiple reflections caused by the irregular surface (multipath).

Measured amplitudes of the first echo varied between  $10mV$  and  $240mV$  depending on the exact position of the transducers.

### 3.2.2.9 Tar - 8cm



**Figure 3-20: Tested surface and received signal - Tar**

Once again, because of the high intensity of the solar light, it was not possible to obtain pictures with acceptable quality.

This surface experiences the same problems described in the previous section, although in a lesser extent.

Measured amplitudes of the first echo varies between  $100mV$  and  $480mV$  depending on the exact position of the transducers.

### 3.2.3 Obtained results with the sensors tilted relative to the ground

The following measures were taken on linoleum using the same signal described previously driving the emitter. The objective was now to evaluate the behaviour of the ultrasounds in different angles relative to the ground's perpendicular.

#### 3.2.3.1 0 degrees – perpendicular to the floor



Figure 3-21: Response at 0 degrees

- Amplitude of the first echo:  $V_{pp} \cong 305mV$

#### 3.2.3.2 22.5 degrees

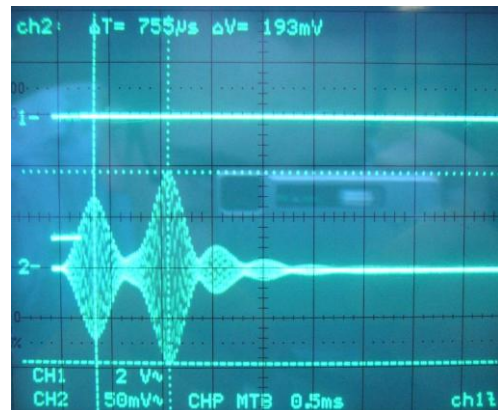


Figure 3-22: Used test setup and obtained response at 22.5 degrees

- Amplitude of the first echo:  $V_{pp} \cong 193mV$

### 3.2.3.3 45 degrees

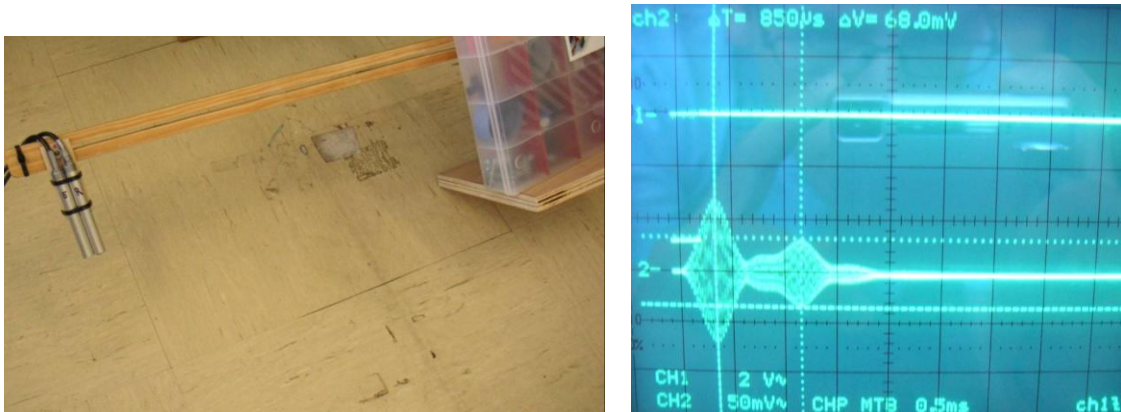


Figure 3-23: Used test setup and obtained response at 45 degrees

- Amplitude of the first echo:  $V_{pp} \cong 68mV$

### 3.2.3.4 65 degrees

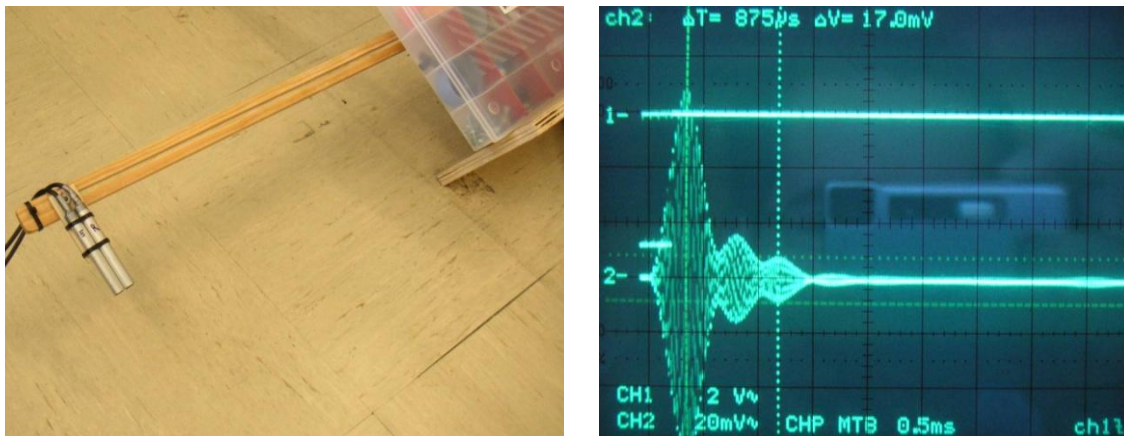


Figure 3-24: Used test setup and obtained response at 65 degrees

- Amplitude of the first echo:  $V_{pp} \cong 17mV$

For angles above 45 degrees, the amplitude of the response starts to decrease rapidly and after 60 degrees the changes of the amplitude are rather small.

### 3.2.4 Acoustical direct path

As mentioned earlier, with this setup, an acoustical direct path (similar to crosstalk) between the ultrasonic emitter and the receiver caused an undesired signal to appear in the response. To better understand why exactly this was happening and if it would be possible to reduce this effect, a simple test was conducted.

In the following, the emitter was driven with an amplitude of  $20\text{ Vpp}$  and the sensors were placed perpendicular to the floor,  $30\text{cm}$  high.

It was found that when a piece of paper was inserted between the emitter and the receiver, the signal component due to the direct path was highly attenuated.

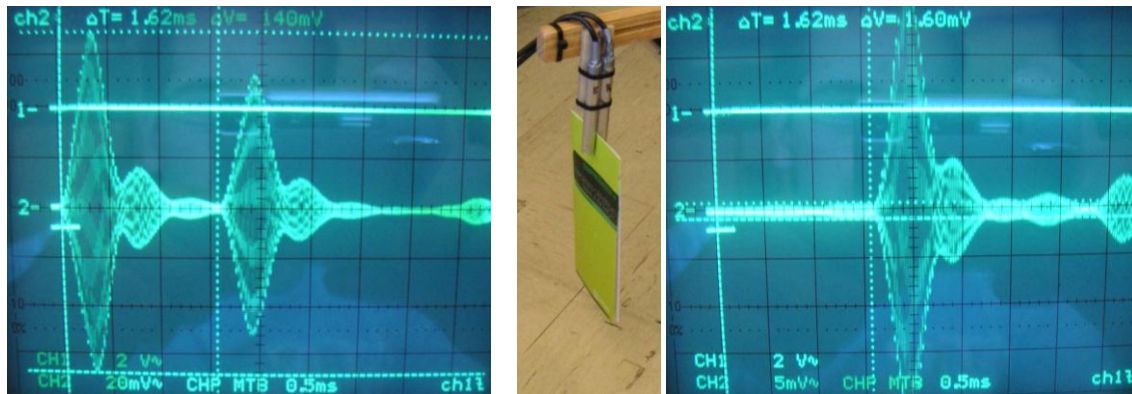


Figure 3-25: Received signal without and with a paper inserted

In a brief observation of obtained responses (Figure 3-25), it is evident that this method, although very simple, proved to be quite effective, reducing the “crosstalk” amplitude almost 100 times, from  $140\text{mVpp}$  to  $1.6\text{mVpp}$ .

### 3.2.5 Use of 4.5 Vpp do drive the emitter

The real circuit will ideally be powered by two AAA rechargeable batteries, having a nominal voltage of  $1.2\text{V}$  each. Thus, the maximum available voltage to drive the emitter would be around  $4.8\text{V}$  ( $2.4\text{V}$  from the batteries that can be doubled by a capacitor in series with the emitter). There was a need to test the behaviour of the ultrasounds in these conditions to better evaluate the viability of their use in a low voltage application.

The following tests were conducted with the same  $300\mu\text{s}$  burst but now with amplitude of  $4.5\text{V}$ . Only carpet and linoleum were tested at different heights.

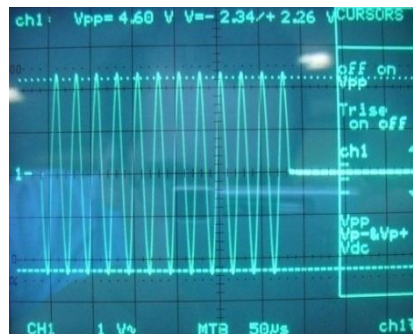


Figure 3-26: Driving signal with 4.5V

### 3.2.5.1 Linoleum - 30cm

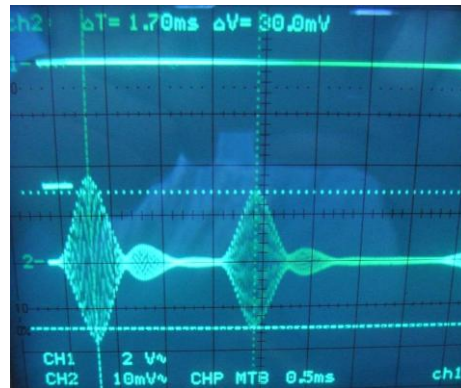


Figure 3-27: Response to the 4.5V signal - linoleum at 30cm

- Amplitude of the first echo:  $V_{pp} \cong 30\text{mV}$

### 3.2.5.2 Carpet - 30cm

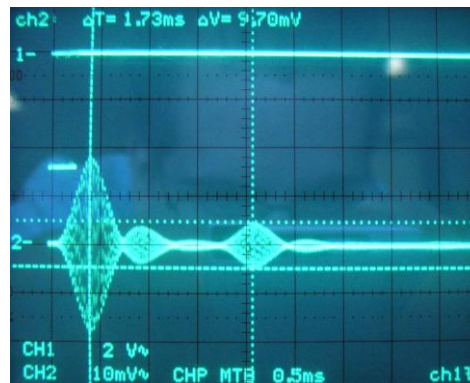


Figure 3-28: Response to the 4.5V signal - carpet at 30cm

- Amplitude of the first echo:  $V_{pp} \cong 9.7\text{mV}$

### 3.2.5.3 Linoleum - 10cm

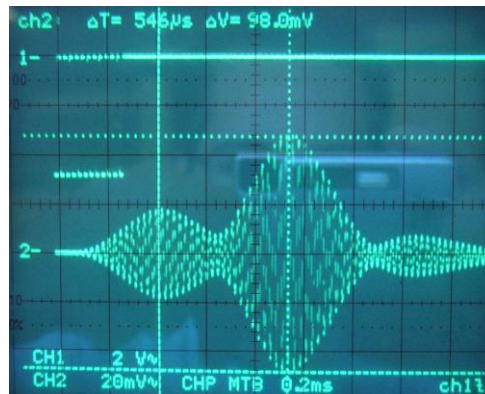


Figure 3-29: Response to the 4.5V signal - linoleum at 10cm

- Amplitude of the first echo:  $V_{pp} \cong 98mV$

### 3.2.5.4 Linoleum - 50cm



Figure 3-30: Response to the 4.5V signal - linoleum at 50cm

- Amplitude of the first echo:  $V_{pp} \cong 16.5mV$

As it can be seen on the previous responses, the received echoes are still very acceptable, showing that an implementation with a low voltage circuit and microcontroller is feasible.

### 3.2.6 Variation of the pulse width

The objective of this test was to evaluate the influence of the driving pulse width in the received echo. The goal is to find a good compromise between the time and energy spent sending the pulse (which should be as low as possible) and the amplitude of the received echo (desired to be as high as possible). The amplitude of the driving signal was set to  $4.5V_{pp}$ , the surface was linoleum, and the sensors were  $20cm$  perpendicular to the floor.

#### 3.2.6.1 300us (12-cycle burst at 40 kHz)

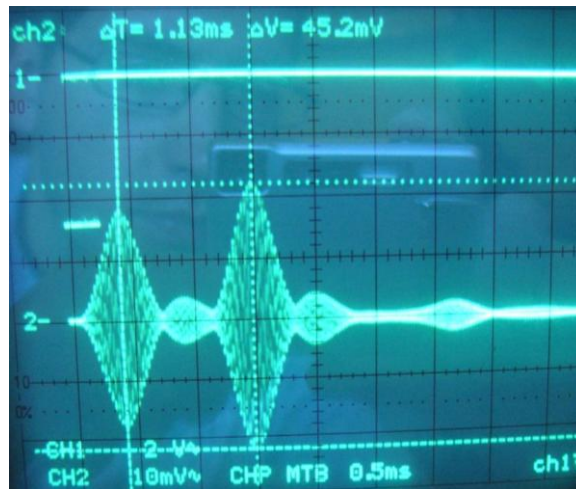


Figure 3-31: Response to a 300 $\mu$ s burst

- Amplitude of the first echo:  $V_{pp} \cong 45.2mV$

#### 3.2.6.2 450us (18-cycle burst at 40 kHz)

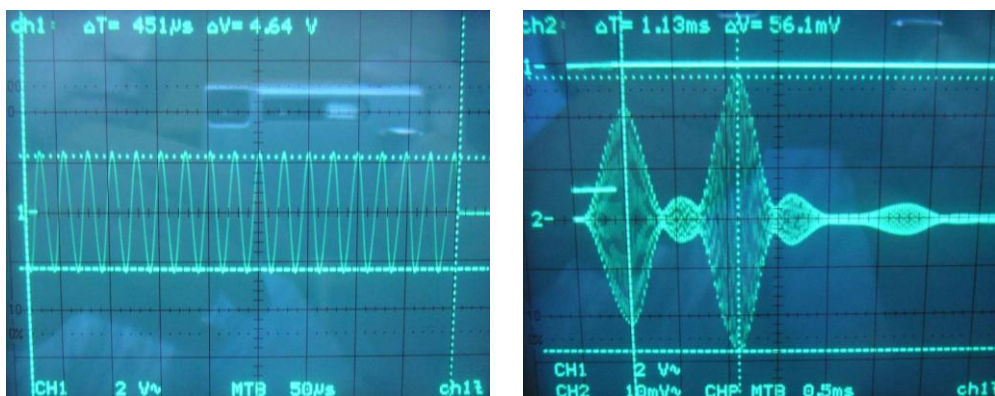


Figure 3-32: Response to a 450 $\mu$ s burst

- Amplitude of the first echo:  $V_{pp} \cong 56.1mV$

### 3.2.6.3 200us (8-cycle burst at 40kHz)

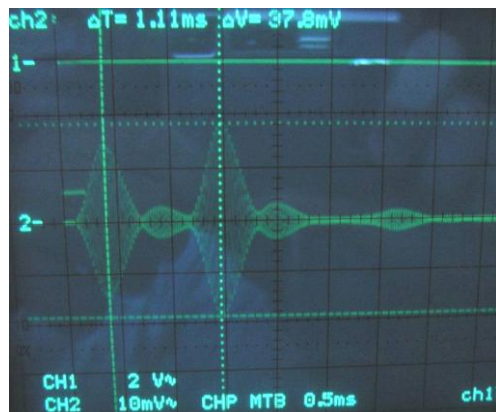


Figure 3-33: Response to a 200 $\mu s$  burst

- Amplitude of the first echo:  $V_{pp} \cong 37.8mV$

### 3.2.6.4 150us (6-cycle burst at 40kHz)

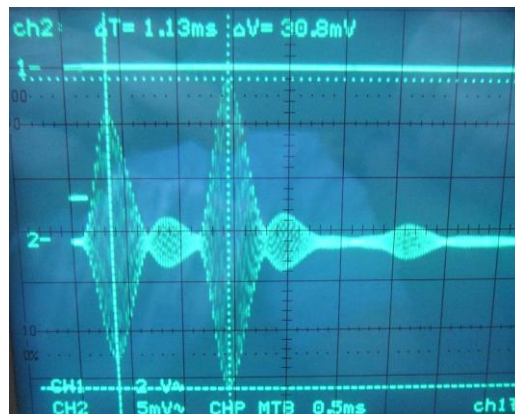


Figure 3-34: Response to a 150 $\mu s$  burst

- Amplitude of the first echo:  $V_{pp} \cong 30.8mV$

### 3.2.6.5 100us (4-cycle burst at 40kHz)

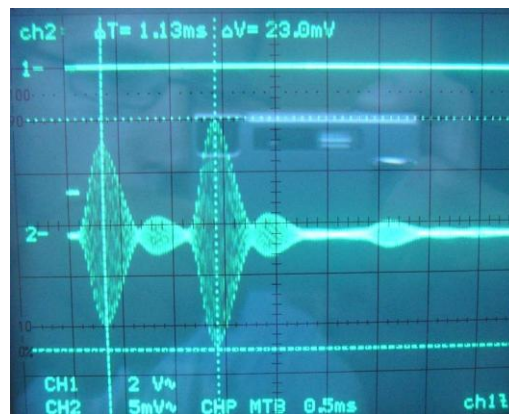


Figure 3-35: Response to a 100 $\mu$ s burst

- Amplitude of the first echo:  $V_{pp} \cong 23mV$

### 3.2.6.6 50us (2-cycle burst at 40kHz)



Figure 3-36: Response to a 50 $\mu$ s burst

- Amplitude of the first echo:  $V_{pp} \cong 14.2mV$

### 3.2.7 Conclusions – problems encountered

Factor to evaluate	Surface	Angle to the floor's perpendicular (degrees)	Distance (cm)	Emmitter driving voltage (Vpp)	Pulse width at 40kHz (μs)	Max. amplitude of the response (first echo) (mVpp)
Type of surface	Linoleum	0	10 - 11	20V	300	305
	Carpet	0	10 - 11	20V	300	70
	Tile	0	10 - 11	20V	300	330
	Rubber #1	0	10 - 11	20V	300	240
	Stone	0	10 - 11	20V	300	349
	Rubber #2	0	10 - 11	20V	300	385
	Irregular - rubber and metal	0	11 - 14	20V	300	214
	Portuguese paving	0	20	20V	300	10-240
	Tar	0	8	20V	300	100-480
Angle	Linoleum	0	10	20V	300	305
	Linoleum	22.5	-	20V	300	193
	Linoleum	45	-	20V	300	68
	Linoleum	65	-	20V	300	17
Voltage driving the emitter	Linoleum	0	30	4.5V	300	30
	Carpet	0	30	4.5V	300	9.7
	Linoleum	0	10	4.5V	300	98
	Linoleum	0	50	4.5V	300	16.5
Pulse width	Linoleum	0	20	4.5V	300	45.2
	Linoleum	0	20	4.5V	450	56.1
	Linoleum	0	20	4.5V	200	37.8
	Linoleum	0	20	4.5V	150	30.8
	Linoleum	0	20	4.5V	100	23
	Linoleum	0	20	4.5V	50	14.2

**Table 2: Summary of the factors that affect the ultrasounds response**

Overall, the obtained results can be considered satisfactory, showing that in most situations no major problems are to be expected. Nonetheless, there are a few specific issues concerning very irregular surfaces like the Portuguese paving. In this kind of surfaces, ultrasound beams experience

multiple reflections, known as multipath. This effect will be addressed in the following section. The acoustical direct path was also one of the problems detected but it does not represent a very concerning issue and can be easily diminished.

This 12-cycle burst was chosen because it represents the minimum value for which there was no sharp decrease in the amplitude of the received signal at a given distance. For longer bursts, it was verified that the gain in the echoes amplitude started to be less significant and that the received signal started to get wider in time. It is important to find the minimum acceptable burst time because it directly concerns the power consumption and the minimal detectable distance as well as it will involve less processing time and memory from a future microcontroller implementation.

Another important subject to highlight concerns the encouraging results when using low voltages to drive the emitter. It was vital to succeed in this particular test due to the compromise of using low-power and low-voltage circuits and microcontroller. As desired, it will be possible to power up the cane with only two AAA rechargeable batteries.

### ***3.3 The multipath effect***

One very problematic issue encountered concerns the multipath effect. This happens when the surface being measured is very irregular, leading to multiple reflections.

Multipath is a propagation phenomenon that results in echoes reaching the ultrasonic receiver by two or more paths.

The effects of multipath include constructive and destructive interference, and phase shifting of the signal. As a result of these effects, sometimes the signal disappears completely due to addition of different phased signals, coming from different paths. When the delay between the multiple reflections is smaller than the pulse width, then it is not possible to distinguish each component, leading to a wider received pulse. The presence of multipath can be observed on Figure 3-18 where due to the irregular reflection surface, the received pulse has a width of  $800\mu\text{s}$  when for a pulse reflected by a flat surface as in the Figure 3-15, the received pulse has a width of  $600\mu\text{s}$ .

#### ***3.3.1 Effects on the pulse detection***

As said above, multipath effects sometimes cause the signal to completely disappear because of the addition of different phased signals, coming from different paths originated by irregular surfaces. This is undoubtedly the worst problem encountered concerning the echoes detection in different surfaces. Signal processing techniques had to be used to try to overcome this difficulty. This cancellation of the echo, if not correctly detected, forces the cane to assume that there is actually no echo due to a hole, issuing therefore a false hole-detection. Another practical effect, which is easily visible when multipath occurs, is the widening of the received pulse. This happens because several echoes arrive in slightly different time instants, although without the cancelling effect from the previous case. Some examples of received sequences of pulses from irregular surfaces are presented in the following pictures.

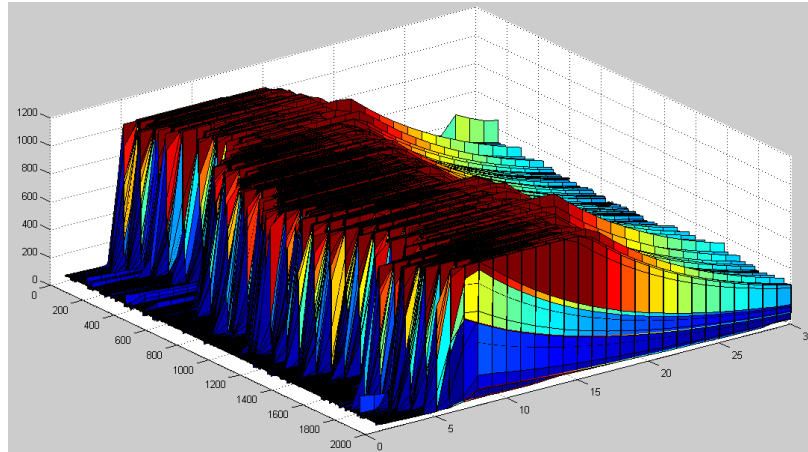


**Figure 3-37: Received pulses from Portuguese paving**

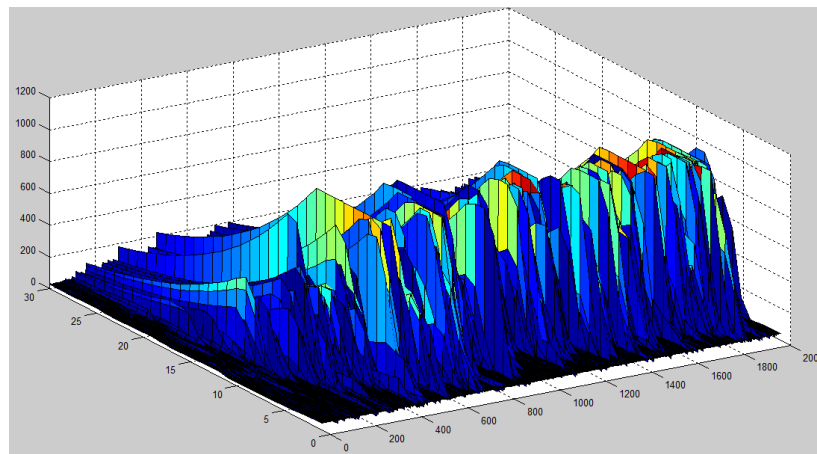


**Figure 3-38: Received pulses from grass**

As it is clear from the pictures, the pulses that should be represented in an almost a continuous image are, instead, a very unstable image with a massive amount of zeros and variations in the amplitude of the echoes.

### ***3.3.2 Using two sensors to create spatial diversity and mitigate the multipath problem***

A diversity scheme refers to a method for improving the reliability of a signal by utilizing two or more channels with different characteristics. Diversity plays an important role in combating fading and co-channel interference and avoiding errors. It is based on the fact that individual channels experience different levels of fading and interference. Multiple versions of the same signal may be transmitted and/or received and combined in the receiver. Diversity techniques improve the losses introduced by the multipath effect.

In order to create diversity in the system and greatly reduce the disappearing of the echoes due to multipath signal cancellation, it was decided to use two ultrasonic receivers, one at each side of the

emitter, slightly separated from each other. One of the receivers was also placed  $1/4$  of the wavelength of the signal higher than the other receiver. With this configuration, when the *zero amplitude* of a signal arrives at the first receiver, the second (higher) receiver will capture a maximum (or minimum) of the same wave, and vice-versa.

Considering the signal frequency  $f$  to be 40kHz, and the speed of sound in air  $c=344m/s$ , one can calculate the wavelength  $\lambda$  according to the following formula:

$$\lambda = \frac{c}{f} = \frac{344}{40} = 8.6mm$$

Thus,  $\frac{\lambda}{4} = 2.15mm$ , and this will be the difference between the heights of both ultrasonic receivers.

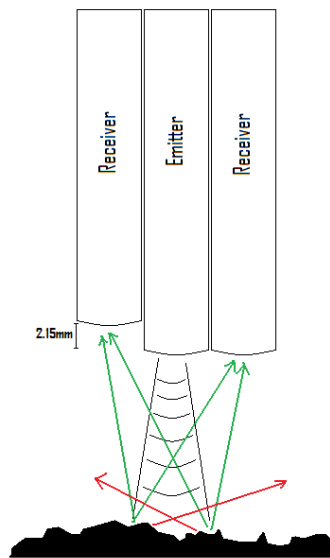


**Figure 3-39: Placement of the sensors and example of multipath**

These techniques introduce spatial diversity in the system and try to mitigate the problem of echo cancellation due to multipath. The probability of having echo cancellation in both received signals is now considerably smaller than if using only one receiver.

### ***3.3.3 Pulse averaging to solve the multipath problem***

Unfortunately, but as expected, the previous diversity techniques were not enough to effectively solve the multipath problem on their own. Therefore, after combining the signals received from both ultrasonic receivers, pulse averaging was applied and IIR filters were used. The use of these filters combined with diversity greatly improved the correct detection of the ground, successfully reducing the multipath effect on irregular surfaces.

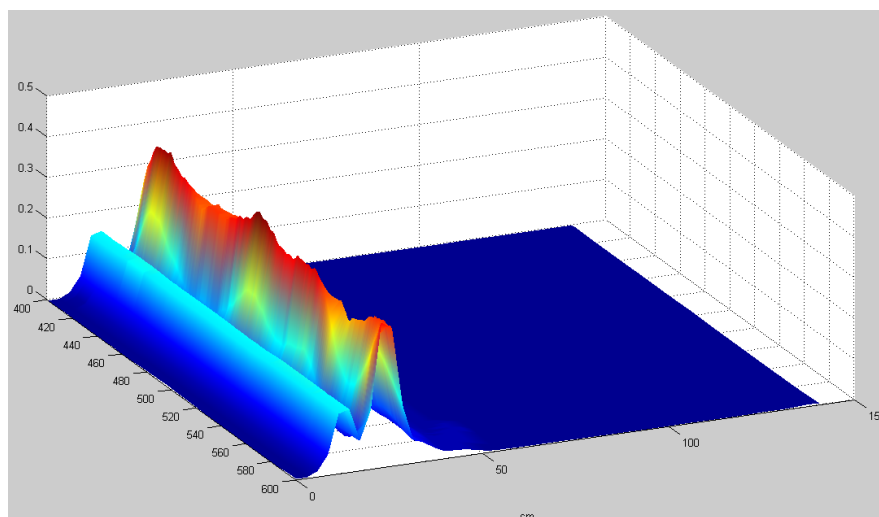


**Figure 3-40: Example of a sequence of pulses after processing**

In the particular case of this picture, the first lump corresponds to the “crosstalk” between sensors and the second lump represents the received echoes. The improvements from the previously showed pictures are evident. All the zeros that appeared were successfully eliminated.

The results obtained were quite promising. More details about the implemented filters will be given in the following chapters.

### ***3.4 Hole-detection algorithm***

Before building the entire prototype, it was imperative to test the feasibility of hole-detection techniques and algorithms, already taking into account the solutions discussed in the previous sections. To do this, an electronic module was developed using a microcontroller, ultrasonic transducers, analogue filters, RS232 serial communication, and a few more components, with the objective of automatically and continuously send pulses of ultrasounds, read the echo of each pulse, convert it to a digital form, and send it to the PC. In the PC, Matlab was used to receive the values of the echoes for further analysis. This allowed for a straightforward and efficient way to develop the algorithms needed to identify the echoes, process them, and identify holes, steps and drop-offs. The physical setup used for the ultrasonic transducers was the same used in section 3.2.1 (page 43) but with the addition of a second receiver as described in section 3.3.2 (page 63). The electronic module developed is the one described in section 4.2 (page 71) but programmed to execute the previously described tasks. More about the module will be presented and can be consulted in section 4.2.

Once in the prototype development stage, this algorithm was then adapted and translated to be implemented entirely in the module’s microcontroller.

#### ***3.4.1 Concept***

The following flowchart shows the concept of the algorithm developed.

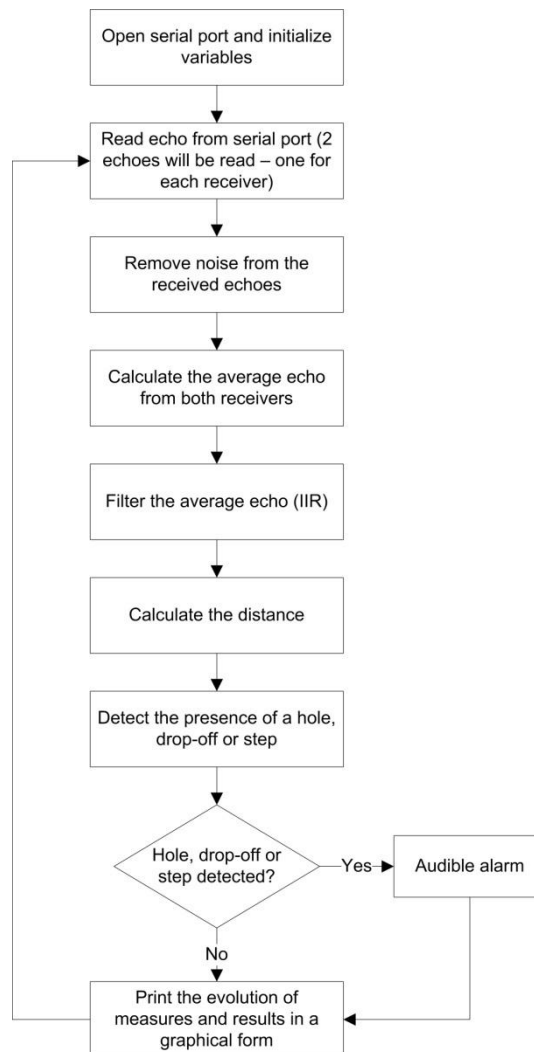


**Figure 3-41: Conceptual flowchart of the hole-detection algorithm developed in Matlab**

Each block will be addressed with more detail in the next section.

### **3.4.2 Description**

The program (in Matlab) starts by cleaning the workspace, opening the serial port with the required configurations, and initializing the variables and arrays that will be used throughout the program’s execution.

When the microcontroller of the electronic module is started, it produces a 40kHz wave with the duration of 300µs. This generates the pulse that will drive the ultrasonic emitter. After sending the pulse, the microcontroller’s ADC will read and convert the received echo from each ultrasonic receiver into a digital form. The picture bellow shows a received pulse at the input channel of the ADC. The ultrasonic sensors were placed at 27cm from the floor.

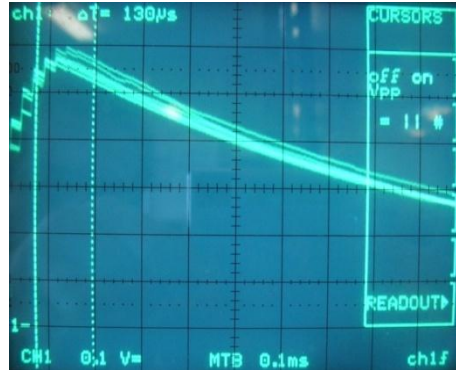


**Figure 3-42: Received echo at the input channel of the microcontroller's ADC**

As can be seen in the picture, the maximum voltage is around 0.58V and in order to have a sample of this signal near the maximum, the sampling period must be at least around 130µs. Thus, a sampling frequency of 10kHz was used, corresponding to a sampling period of 100µs. If the maximum distance (from the sensors to the floor) that is required to be read is 50cm (after this it can be considered that a deep hole is underneath the cane), then 30 samples at 10kHz will be required in the ADC to accurately read a received echo.

$$d = v \times t$$

$$t = \frac{d}{v} = \frac{0.5m \times 2}{343m/s} = 2.915ms \cong 3ms$$

$$N_{ADC \text{ samples}} = \frac{3ms}{100\mu s} = 30 \text{ samples @ } 10kHz \text{ (for } 50cm)$$

Thus, the ADC will read and convert 60 samples for each emitted pulse, 30 per each receiver, and send these samples with the respective identification of the corresponding receiver to the PC via the RS232 serial port. The microcontroller then produces a new pulse and follows the same steps described in a loop. It should be noted that every time the microcontroller is not directly required for an operation, it is put into a power saving mode.

The software in Matlab then reads and validates the received echo from each ultrasonic receiver, making sure that both blocks of 30 samples corresponding to each receiver were correctly read. If any error is detected, it discards these values and reads a new pair of echoes.

When in the presence of valid readings, the software then proceeds by removing some noise that was detected to be always present in the received echoes. This noise was found to be almost time invariable, although different in each receiver channel, and is probably due to crosstalk and interferences in the PCB lines, even though ground planes were used to minimize these effects. The characterization of this noise is presented in Appendix D, in page 103.

The next step is to simply calculate an average of the echoes received by both channels.

It then applies a low-pass IIR filter to this new echo average, where:

$$Echo_{filtered} [n] = (1 - \alpha) \times Echo_{Average} + \alpha \times Echo_{filtered} [n - 1]$$

Being  $\alpha$  the filter's coefficient, that was set to 0.9.

The use of this filter smoothes the response and eliminates many errors due to sudden echo cancelations, with the drawback of slightly slowing down the evolution of the response when in the presence of a hole, drop-off or step. The value  $\alpha = 0.9$  presented a good compromise between speed and smoothing.

The algorithm then calculates the actual distance to the floor by finding the sample that corresponds to the maximum amplitude of the filtered echo. Once the number of the sample is known, it is easy to obtain the distance to the floor: as demonstrated earlier, 30 samples (3ms) correspond to a distance of 50cm, so the maximizing sample will correspond to

$$Distance = Sample_{index} \times \frac{50}{30}$$

If no echo is detected consecutively over a small period, the maximum distance (50cm) is assumed.

The next step is to evaluate if the cane is passing over a hole, step or drop-off. The algorithm does this evaluation based on two separate methods. The first method is to detect sudden variations in the distance between the sensors and the floor. To do this, a weighed differentiator filter is used so that small variations due to instability or inaccurate readings are filtered, and a threshold was set for this derivative above which a hole, drop-off or step is detected. The impulse response of this filter is:

$$H_n = [-1, -1, -1, -1, -1, 0, 0, 1, 1, 1, 1, 1]$$

It multiplies the last 12 samples of the calculated distance by the corresponding weight of the filter position ("-1", "0" or "1"), and then adds the 12 attained values. As higher the slope of the distance variation, the higher the value given by the filter will be. The objective was to find the first derivative of the distance variation, which could not be calculated with the usual method of using only the last two samples because many sudden small variations (without meaning) would be detected.

A simple example of the results attained using this filter is depicted in the next picture, showing that only consistent changes in the distance are effectively amplified (detected). The blue line corresponds to the variation of the distance and the green line is the output of the differentiating filter.

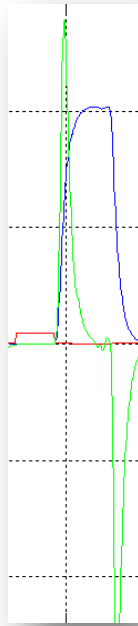


**Figure 3-43: Example of the method for calculating the slope of the distance variation**

Whenever a new sample (distance) is introduced, the algorithm calculates the corresponding slope (difference) and makes a decision based on the absolute value of the obtained result, comparing it with a threshold that was set to 30 (experimentally tested). If the value is higher than the threshold, it detects a hole, drop-off or step.

The drawback of this method is that it slightly retards the detection of a hole, because as can be seen in the figure, the abrupt change in the distance will only be detected after a few more samples. This delay is even bigger if in the presence of a very deep hole, higher than the maximum detectable 50cm, because there will be no received echo and the filter will take more time to lower the response from the previous echoes. Thus, in order to improve this delay and complement the hole-detection, a second method was developed that analyses the changes in the maximum amplitude of the averaged and filtered echoes. With this, in situations where there is a change between a strong echo and no echo at all (a very deep hole), where the filter would take some time to lower the response, not originating a sudden variation of the calculated distance (the distance is calculated using the maximum amplitude of the echo, which in the absence of a new echo keeps the same form, although it's amplitude starts to decrease) a hole will still be detected due to the slope of the amplitude's variation. This method uses exactly the same algorithm described above to differentiate the signal but now with the objective of detecting sudden changes in the maximum amplitude of the received echoes. Its threshold was set to 1800, after which a hole, drop-off or step is detected.

A more detailed analysis of this method, as well as a comparison with the previous method is presented in 0 (page 107) and should be consulted.

After this step, the algorithm simply sounds an alarm if a hole, drop-off or step was detected, presents the evolution of the measurements and results in a graphical form, and proceeds to the beginning of the loop, reading a new pair of echoes for further processing.



## **4 Hole-detecting cane**

Based on the feedback obtained from the visually impaired association and the lack of a strong and effective alternative in the market, combined with the results from preliminary tests of the ultrasounds as well as some personal new ideas, a vision of what the cane should be and which features it should incorporate started to come into sight. This new hole-detecting cane would have ultrasonic sensors on the tip, high brightness LEDs along the body of the cane, a solar panel to charge the batteries and detect the ambient light, vibration and audio feedback and, of course, it should be as low-cost as possible and with the lowest possible power consumption. Due to these last two requirements, many compromises had to be done concerning the price, availability, functions, and power consumption of each component. The cane should also be as light as possible and the batteries should last long enough so that the user should not have to worry about them in a regular basis.

The main goals of the cane would thus be to detect holes, drop-offs and steps, improve the users' safety and visibility among traffic and employ mostly vibrations so that it will not interfere with the users' perception of the environment sounds.

### ***4.1 Development of the cane***

The development of the hole-detecting cane was divided in two major modules that could, afterwards, be interconnected or combined into a single circuit. One of these modules would specifically focus on the hole-detection task, incorporating the development of all the hardware and algorithms needed to correctly manage the ultrasounds and apply signal-processing techniques to accurately identify holes, drop-offs and steps on the floor. The other module would address all the hardware and software concerning the power management and supply, the detection of the luminous intensity of the environment and consequent control of the safety LEDs, the audio and tactile feedback and the interface with the user.

This division of features and tasks into two separate modules occurred because although the whole development of the cane started with the ultrasounds module, the power management module was developed in parallel as the final project of an optional course in low-power electronics. This module was thus developed also under the guidance of Prof. Dr. Rui Manuel Escadas Ramos Martins, from the electronics department of the University of Aveiro.

### ***4.2 Module #1 – Ultrasound control and hole-detection***

This module is responsible for the hole-detection task. It concerns all the hardware and algorithms needed to correctly manage the ultrasounds and the development of signal-processing techniques in order to accurately identify holes, drop-offs and steps on the floor.

A note must be made concerning the microcontroller used in this module. The entire module was first developed using a MSP430F2012 from Texas Instruments, but in a later development stage, it was replaced by a MSP430F2274 integrated in the eZ430-RF2500 development tool, also from Texas Instruments. This change was especially due to greater memory capacity, more available external pins, integrated UART, and the inclusion of wireless capability for possible future implementations.

### 4.2.1 Global module description

A block diagram of this module is presented in Figure 4-1.

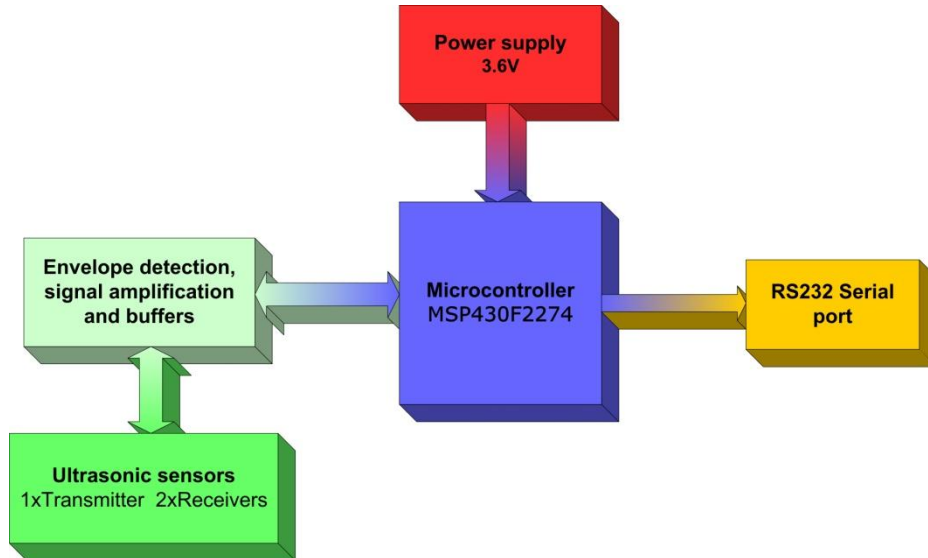


Figure 4-1: Block diagram of module #1

The purpose of this module is to generate the pulses of ultrasounds to be transmitted, receive the respective echo, filter this echo, detect its envelope, and then use software with signal processing techniques to analyse several successive envelopes so that holes, drop-offs and steps can be detected.

Once again, low-power and low-cost were important requirements.

As said previously, this module was firstly designed with the MSP430F2012, and later adapted to the MSP430F2274. To do this, a flat cable was used to match the pins of the new microcontroller with the corresponding pins of the previous one. With this change, only the circuit of the RS232 interface had to be externally redesigned due to pin incompatibility, to the desired higher transmission speeds and lower power consumption. Further specific details will be given in the following sections.

The signal processing and hole-detection algorithms were first developed using Matlab (section 3.4 of page 65) until acceptable results were attained. Then, these algorithms were adapted and translated into C language and implemented in the microcontroller. This approach allowed using a faster development and debugging environment, without memory restrictions and other limitations inherent to microcontrollers. Received pulses could thus be easily seen instantaneously in a graphical way, and the values stored for further analysis. Ultrasound pulses were generated by the microcontroller, which also received the envelopes of the echoes.

Included in this module are also a speaker, three LEDs and two push buttons designed mainly for debug purposes and for possible future needs.

This module was placed inside a metal box, for noise and interference shielding as well mechanical protection. In this prototype stage, this module was designed with the intention of being carried

outside the cane, in a waist-bag or backpack, and to be externally connected with module #2. This leaves the miniaturization issue for later improvements and simplifies the prototype development.

The circuit's schematic and the PCB of this module are presented in Figure 7-2 (page 96) and in Figure 7-5 (page 99) respectively.

## 4.2.2 Block-wise description

Details about each block are given in the following sections.

### 4.2.2.1 Microcontroller

The microcontroller used for this module, MSP430F2274, is very similar to the one used in module #2 (MSP430F2012) but incorporates more and improved features. Two of the most important improvements of this unit are the available memory of 32KB of flash memory and 1KB of RAM against the 2KB of flash memory and 128B of RAM from the MSP430F2012, as well as the inclusion of the UART interface.

Among other features, this microcontroller has a Low Supply Voltage Range of 1.8 V to 3.6 V, internal frequency generation up to 16 MHz, Ultralow-Power Consumption of 270  $\mu$ A (at 1 MHz, 2.2 V) in the Active Mode, 0.7  $\mu$ A in Standby Mode and 0.1  $\mu$ A in Off Mode (RAM Retention), Ultrafast Wake-Up from Standby Mode in less than 1  $\mu$ s, and a 10-Bit, 200-ksp/s ADC with Internal Reference and Data Transfer Controller.

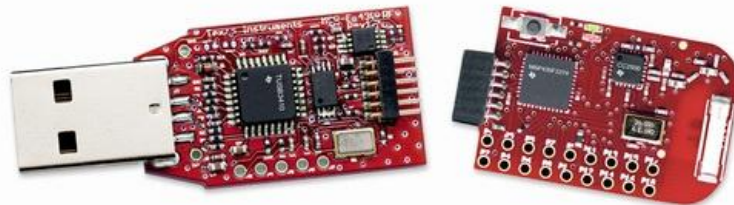


**Figure 4-2: ez430-RF2500 Development Tool**

The picture above shows the ez430-RF2500 development tool from Texas Instruments with the USB interface for programming, debugging and communication, followed by the target board with the microcontroller and wireless circuits. A small drawback of this target board is that the microcontroller's external clock pins are already assigned and interfaced with other pins from the wireless chip, making it impossible to use an external crystal oscillator, important for an accurate generation of the 40kHz wave. For this reason, the internal low-power digitally controlled oscillator of the microcontroller had to be used which although not as accurate as an external crystal oscillator, can perform very well, provided that the supply voltage does not change and keeps a stable value.

#### 4.2.2.2 Power supply

Due to the impossibility of using an external crystal oscillator in the MSP430F2274 development board, the integrated low-power DCO of the microcontroller had to be used. The oscillating frequency of this basic oscillator is highly dependent on the supply voltage although relatively stable over temperature variations. For this reason, a regulated supply had to be used, keeping a stable voltage of 3.6V to the circuit independently of changes in the batteries voltage.

The reason why it is so important to achieve a precise and stable frequency is due to the frequency response and bandwidth of the ultrasonic sensors. Any slight change away from the nominal 40kHz significantly reduces the power of the transmitted wave (SPL) as well as the receiver's sensitivity.

Two complimentary ways to obtain the regulated voltage were used. When using the module connected to the PC for real time processing in Matlab via the development board, the 5V supplied by the USB port were used and regulated directly by the built-in 3.6V voltage regulator of the development board. This voltage was then supplied to the rest of the circuit. When the module is to be used apart from a computer, i.e. as a portable device, a MAX1675 High-Efficiency, Low-Supply-Current, Step-Up DC-DC Converter from MAXIM was used to achieve a stable 3.6V supply voltage from 2 AAA rechargeable batteries. A very good advantage of this circuit is that it can maintain a stable output of 3.6V even when the input voltage is as low as 0.6V, enhancing the usable battery voltage range between charges. The circuit used for this device is the one suggested in the device's datasheet and is presented in the next picture.

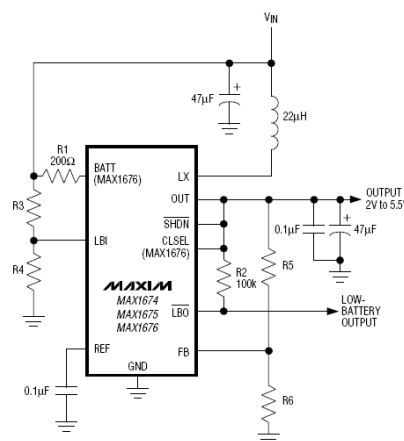


Figure 4-3: Voltage regulation circuit (MAX1675)

Where the only resistors used were  $R5 = 390k\Omega$  and  $R6 = 220k\Omega$  to adjust the output voltage to 3.6V.  $LBI$  and  $\overline{LBO}$  were connected to the ground because the low-battery comparator is not being used.

#### 4.2.2.3 Ultrasonic sensors

The ultrasonic sensors used for the development of this module were the Murata MA40S4T/R. These sensors had already been tested and characterized in section 3.2. They were chosen due to the great balance between price, performance and size that they present.

One ultrasonic emitter and two receivers were used to create spatial diversity, as already explained in section 3.3.2. Once again, they were placed inside small aluminium tubes for electromagnetic shielding so that noise and interferences can be reduced. The receivers were placed with a

difference in their heights of  $\frac{1}{4}$  the wavelength of the 40kHz pulse frequency to help mitigating multipath effects. Coaxial cables were used to carry the electric signals between the sensors and the circuit.

Receiving and driving circuits of the ultrasonic sensors are presented in the module #1 circuit schematic of Figure 7-2 in page 96.

#### ***4.2.2.4 Envelope detection, signal amplification and driving method***

In order to make the received pulses easily readable by the microcontroller's ADC, they had to be rectified, amplified and envelope detection was applied to the 40kHz received wave. To do this, a rectifying circuit with amplification followed by a low pass filter was used in each receiver.

To drive the ultrasonic emitter, a configuration with buffers and a capacitor was used so that the amplitude of the applied signal at the sensor's terminals is almost doubled.

These circuits are presented and should be consulted in Figure 7-2: Electrical schematic of module #1 (page 96) of Appendix A.

#### ***4.2.2.5 RS232 Serial port***

A serial RS232 port was used for communications between this module and a PC. The interface that had been designed with the previous microcontroller (which did not include UART communication interface) was not suitable for the new microcontroller due to pin incompatibility. Thus, a new external circuit was designed with an improved transceiver (MAX3238) that presented lower power consumptions, higher transmission speeds (230.4kbps was the used speed) and auto-power-down feature. This simple circuit directly connects to the UART interface of the microcontroller and to any RS232 serial port of a PC, allowing sending data reasonably fast, for real time processing in Matlab. The circuit schematic is presented in Figure 7-3 (page 97) and the PCB in Figure 7-6 (page 100).

### ***4.2.3 Software***

The main purpose of this module's software is to control the emission of the ultrasonic pulses, read and analyse the received echoes, determine if a hole, drop-off or step was detected, and communicate with module #2 to turn it on or off and to control the vibration motor when holes are detected.

The software implemented in this module's microcontroller has the same algorithm that was developed previously with Matlab, presented in section 3.4 of page 65. Please consult that section for details about the hole-detecting algorithm. The Matlab code was translated into C language and adapted for the specificities of the system and of the microcontroller. Once again, and whenever possible, the microcontroller was forced to enter low-power modes in order to save as much power as possible.

All the code files are included in the attached CD-ROM.

#### 4.2.4 Developed Hardware

A PCB was designed with all the circuits described earlier and mounted inside a metal box that besides providing electromagnetic shielding also houses the batteries and all the necessary connectors as well as some redundant features as some extra push buttons, LEDs and a speaker that were connected to the microcontroller so that they can be easily used if necessary. During the development of this module there were no space concerns or limitations because as it is still a prototype there were no such requirements. This allows a good and solid PCB design as well as using bigger connectors, which are more robust, and makes it easier to make any necessary changes to the circuits during the development.

The module was also designed to be easily swapped from a test bench (where it could be connected to a PC for programming and analysed with Matlab) to the cane itself, via interconnection with module #2. It also allowed to be easily debugged in real-time using JTAG, being connected at the same time to the PC and to the cane (via module #2).

An ON/OFF push switch was mounted in the case that turns both modules ON or OFF. This switch is especially suited to be used by blind persons because it clearly indicates if the circuit is turned ON or turned OFF. The button is raised when in the OFF position, staying lowered at the box outer wall level when ON.

Except for the connectors of the ultrasonic sensors, which can be intentionally swapped between channels, all the connectors are “poka-yoke”, allowing only one possible way to be connected. Although still a prototype, it would thus be easier for a blind person to make the necessary connections.



Figure 4-4: Module #1



Figure 4-5: Module #1 - front and rear panel

## 4.3 Module #2 - Power, LEDs and feedback

As said earlier, this module intends to implement and control all the hardware and software concerning the power management and supply, the detection of the luminous intensity of the environment and consequent control of the safety LEDs, the audio and tactile feedback and the interface with the user. When developing this block, the higher goals of low-voltage supply and low-power consumption for a long battery life were always kept present.

### 4.3.1 Global module description

The projected and developed system concerning this module is represented in the block diagram of Figure 4-6.

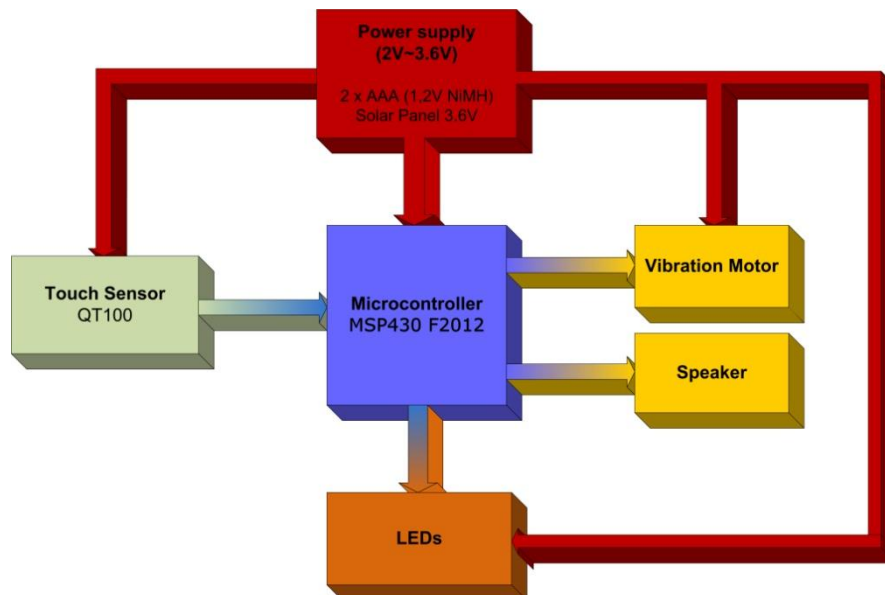


Figure 4-6: Block diagram of module #2

As can be seen in the diagram, the main component of this module is the MSP430F2012 microcontroller from Texas Instruments. This particular model was chosen due to its ultra-low-power consumption, small size, ease of integration, reliability and low-cost, making it very well suited for portable and battery-powered applications.

To power up the circuit, two AAA rechargeable NiMH batteries were interconnected with a solar panel that besides recharging the batteries and powering the circuit when exposed to sunlight, is also used to detect if the cane is being used during the day or night in order to decide if the safety LEDs should or should not be turned on. These LEDs improve the safety of the user near traffic areas by allowing car drivers to see the visually impaired clearly during the night. The flashing LEDs will get the drivers attention and alert them earlier so that they can make any required precautions. The reason why AAA rechargeable batteries were chosen is due their high capacity, low price, availability, ease of replacement and possibility to recharge them outside the cane with any regular batteries charger.

In order to avoid having moving parts in the cane, it was chosen to use a touch sensor instead of a regular ON/OFF switch. Later on, we will see that although interesting, this option proved not to be very effective.

Warnings to the user were given through vibration in the handle of the cane. Different combinations of vibrations were used for different kinds of information. The built-in speaker proved to be slightly ineffective. As it was inside the cane, the sound intensity heard outside was very low. Nevertheless, it can be used for redundant or supplementary information.

### **4.3.2 How the module works**

Whenever the user wishes to turn the circuit on or off, all he needs to do is to touch the area defined by the electrode of the touch sensor for about three seconds. This area is the top cover of the cane. After this, the cane will inform the user about the battery voltage level so that he knows if it will be enough for his journey. To do this, the cane will vibrate and beep between 1 and 5 times, according to the voltage of the batteries. Five times corresponds to a full battery charge and one means that the batteries are almost exhausted. Whenever the solar panel is under direct sunlight, it will automatically start to recharge the batteries.

When the cane is active (turned on), it will evaluate the lighting condition of the environment in order to decide if the safety LEDs should or not be turned on.

Given that the detection of holes does not concern this building block, the vibration due to detection of holes was not implemented at this point. Nevertheless, for demonstration purposes, the vibration motor was activated in predetermined time intervals, vibrating two consecutive times in small bursts.

The cane was never completely turned off because the touch sensor needed to be constantly monitored. It was rather in a very low power mode, where the microcontroller was placed in a deep sleep mode, waiting for an interrupt coming from the touch sensor.

### **4.3.3 Block-wise description**

A more detailed description of each building block of this module will be given in the following sections.

#### **4.3.3.1 Power supply**

To supply the required power to the circuit, two AAA batteries were used combined with a flexible solar panel from *PowerFilm* (model MTP 3.6-150) with a nominal voltage of 3.6V and a maximum current of 100mA. One of the main reasons why this solar panel was chosen is because of its flexibility, allowing it to be placed around the body of the cane. The 3.6V are perfect to charge two 1.2V AAA batteries connected in series, not requiring any additional circuits for voltage conversions, and the 100mA represent the 10% of the batteries capacity (1000mAh) recommended for slow charges, without the risk of overload. Thus, the solar panel can be directly connected to the batteries, provided that only a simple diode prevents the batteries from draining through the panel when in dark places. A low voltage drop diode was used (0.2V) in order to maximize the voltage delivered to the batteries.

The choice of using two 1.2V AAA batteries was based on their relatively small size and weight, low-cost, and high flexibility, because many regular chargers available in the market can recharge them. They are also very easy to find and buy in any supermarket or specialty store, making it easy and cheap to replace when they reach the end of their lives.

#### 4.3.3.2 DC vibration motor

Given the difficulty in finding small DC vibration motors, it was decided to remove, use and test motors from several devices like an Ericsson T28s and a Nokia 8310 mobile phones, a vibrating toothbrush from Oral-B and from another mobile phone of unknown brand and model. The objective was to compare the several motors and chose the one with better characteristics.

The motor from the toothbrush was undoubtedly the one with higher vibration intensity. Nonetheless, it was also the one which consumed more current: about 430mA@2.5V.

Also with an interesting intensity of vibration but still with a prohibitive current consumption was the Nokia 8310 with 210mA@2.5V.

135mA@2.5V was the current drained by the motor of the unknown branded mobile phone, which in turn presented an unsatisfactory intensity of vibration.

The motor from the Ericsson T28s was the one with the most interesting balance between intensity of vibration and current consumption. It presented good vibration intensity with a current of about 40mA@2.5V. This was therefore the selected motor for the cane.

The motor is driven by a VN2222L MOSFET (with 270mA of maximum continuous drain current), which in turn is controlled by an I/O port of the microcontroller. This allows feeding the motor with the maximum voltage and current available (directly from the batteries).

#### 4.3.3.3 Speaker

The idea of introducing a small speaker was to test the use of some audible signals that could complement the vibration. The speaker used was also from the Ericsson T28s phone.

In this first version of the cane, the speaker is only used to signal the entry in the interrupt service routine of the touch sensor and to inform about the battery level along with the vibration motor.

The sound produced by the speaker consists of small bursts of a 440Hz square wave, treated in this text as beeps.

#### 4.3.3.4 Touch sensor

The initial idea behind the use of a touch sensor was to make the cane completely automatic, not requiring any direct user intervention to be turned on or off. It would automatically turn itself on when it sensed that the user was grabbing it, and turn off after some period without detecting the users' hand. This would correspond to the desired operation mode of the touch sensor: when it detects a finger or other body part, it activates an external output pin to logic level "1". When a finger is not detected, a "0" logic level would appear in that same output pin.

Throughout the development phase, it was clear that this behaviour would not be possible. The used touch sensor (a QT100 from *Quantum Research Group*) has a "Max. On Time" of 80 seconds after which the sensor automatically recalibrates itself. Thus, when the user would start using the

cane, it would effectively turn on, but after this “Max On Time” (80 seconds) the touch sensor would auto-recalibrate, outputting a “0” and consequently turning the cane off.

To avoid this situation, the touch sensor electrode was placed on the top cover of the cane and the microcontroller was set to only turn on or off after a minimum period of 3 seconds of continuous touch in this area. This way, the output pin of the touch sensor will normally be “0” changing to “1” only when the user directly touches the area of the electrode, meaning that he wishes to turn the cane on or off. This output pin was connected to an I/O port of the microcontroller, producing an interrupt whenever its logic level changes from “0” to “1”.

Several issues concerning the touch sensor also arise when assembling and testing it. A great care had to be given to ground planes placed near the electrode and its lines because it may produce false detections and reduce the sensibility of the sensor. Any kind of noise near this areas can also lead to the same unwanted effects. This is why coaxial cable was used to connect the sensor to its electrode, avoiding noise and interferences.

The capacitor used to define the sensibility of the touch sensor is of great importance. Its value was obtained experimentally until the desired sensibility was found. This value was 15.6nF and falls into the values range given by the manufacturer. A 6mm thick piece of PVC was used as a dielectric for the electrode, working also as a cap for the top of the cane.

#### 4.3.3.5 LEDs

The LEDs selected for this module were the *TLWR9922 TELUX* developed by Vishay. These high brightness red light LEDs presented a good compromise between price, luminous flux, and viewing angle. The only disadvantage relies in the relatively high nominal forward voltage of 2.7V. However, experimental results showed that even with lower voltages of about 2V, the brightness of the LED was still quite acceptable.

The viewing angle of 90 degrees is of great importance for this application, allowing the LEDs to be seen in almost every direction. Three LEDs were placed on each side of the body of the cane.

Figure 4-7 presents the circuit developed to drive each LED.

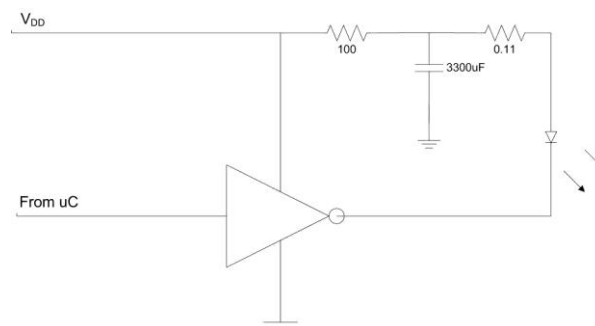


**Figure 4-7: LEDs driving circuit**

This circuit makes it possible to flash the LED without causing disturbances in the power supply lines like drops in the voltage or current peaks that could affect the behaviour of other circuits.

When the circuit is powered on, the large capacitor will charge to  $V_{DD}$ , and when the buffer output drops to “0” the energy in the capacitor will flow through the LED to the ground. The 100Ω resistor limits the charging current of the capacitor preventing abrupt drops in  $V_{DD}$ .

#### 4.3.3.6 Microcontroller

The chosen microcontroller for this circuit was the MSP430F2012 from Texas Instruments, included in a USB development tool called eZ430-F2013, which is very flexible and easy to use (Figure 4-8).

As said before, this microcontroller is especially well suited for mobile and low-power applications. It works with supply voltages between 1.8V and 3.6V, and consumes only  $220\mu\text{A}@1\text{MHz}@2.2\text{V}$  in active mode. Even more interesting are its 5 low-power modes in which it consumes from only  $0.1\mu\text{A}$  and  $0.5\mu\text{A}$ . Important to notice is the ultra fast wake-up from low-power modes of less than  $1\mu\text{s}$ . This very short wake-up time allows using low-power modes between almost any operations that require a small amount of time without the direct need of the CPU.



**Figure 4-8: eZ430-F2013 development tool**

The electrical schematic of the complete circuit of this module is illustrated in page 95, Figure 7-1 of appendix A.

#### 4.3.4 Software

The software implemented in this module is almost completely interrupt driven. Nonetheless, there is a fairly predetermined sequence of execution.

Figure 4-9 presents the global operation flowchart of the software implemented in the microcontroller of module #2. In the following, some specific blocks will be addressed with more detail and some excerpts of code can be consulted in Appendix C, page 101.

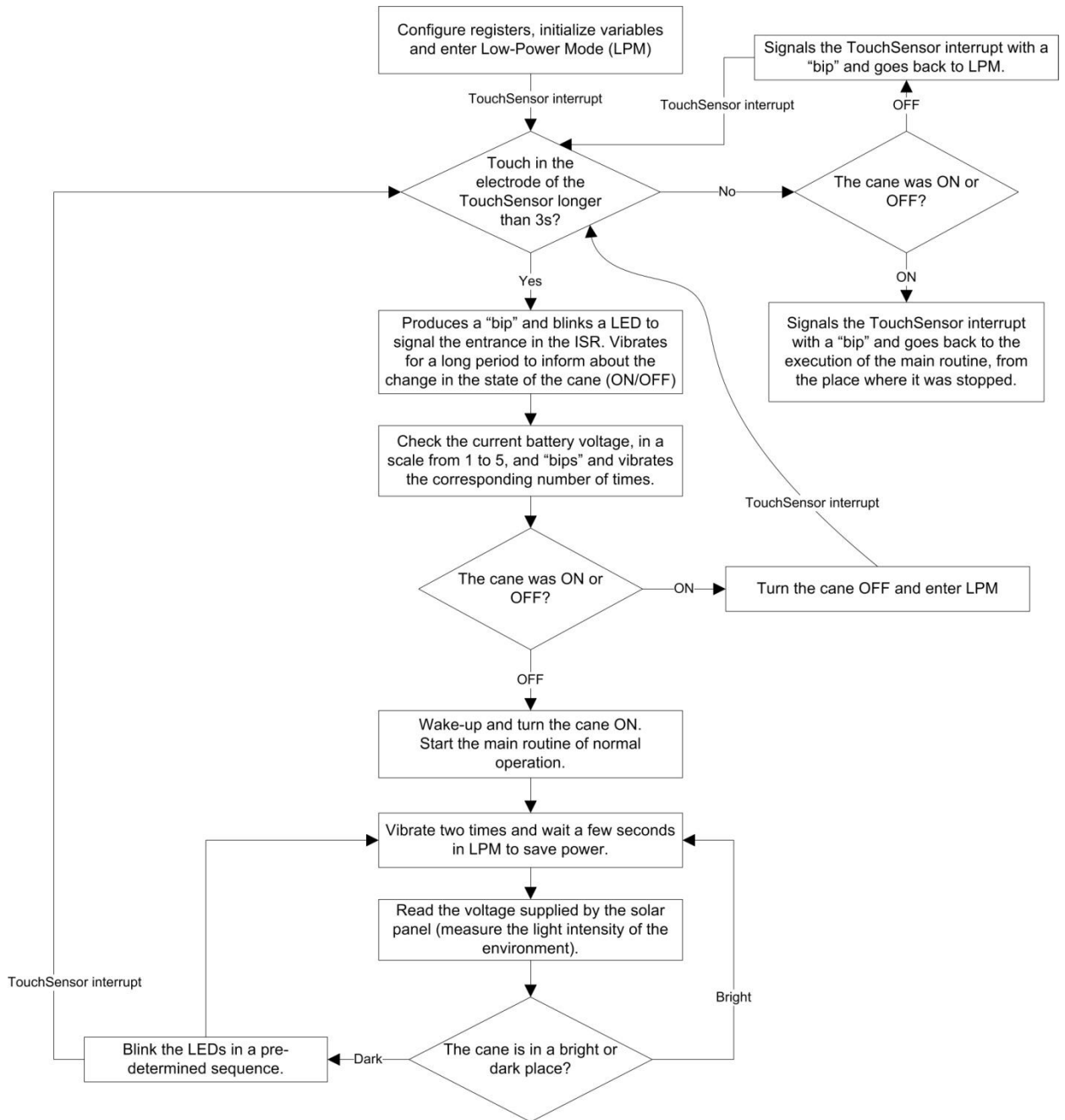


**Figure 4-9: Flowchart of the module #2 microcontroller software**

Although not explicitly stated in the flowchart, in almost every kind of operation that lasts more than a few microseconds, the microcontroller is placed in a low-power mode to save energy. Some examples are settling time of the ADC internal voltage reference, the time between consecutive LED flashes, while the motor is vibrating and while the ADC is converting and saving values into memory, as well as any simple waiting period. Whenever possible, no polling is used. Instead, the microcontroller enters a low-power mode and waits for some interrupt to wake-up. In addition, peripherals are always turned off, unless their operation is actually needed.

#### ***4.3.4.1 Blinking the safety LEDs***

Some portions of the code associated to this task can be consulted in page 101, Figure 7-7 and Figure 7-8.

The LEDs are treated as pairs, top, middle, and bottom. The blinking sequence is as follows (Figure 7-7): first the top pair flashes, after which a timer starts to count and the CPU enters a low-power mode; when the timer reaches the end of some predetermined counts, it wakes up the CPU and the middle LEDs pair flashes. This cycle repeats for the bottom pair, returning to the middle and top pairs once more. It is important to notice that in the whole blinking process, only one LED is activated at a given time. This reduces possible drops in the supply voltage due to high currents peaks.

A very interesting and important feature concerns the way in which LEDs are driven (Figure 7-8). They are not continually activated but instead they are driven by a 5ms long PWM (Pulse Width Modulation) with a duty-cycle of 50% and a frequency of about 37kHz. This method was tested in the laboratory and proved that there was practically no difference, to the human eye, in the brightness of the LED. However, the current consumption was reduced almost to half.

#### ***4.3.4.2 Activation and use of the ADC***

As peripherals are always turned off in order to save power, whenever the ADC is needed it has to be first activated and initialized. This means that the reference voltage must also be set each time the ADC is used. As can be seen in the code of Figure 7-9 (page 102), the CPU waits for the reference voltage to settle in a low-power mode. After this time, the timer wakes it up and the CPU orders the start of the ADC conversion, entering once again in a low-power mode until the end of conversion.

#### ***4.3.5 Proposed prototype of module #2***

An aluminium tube was chosen to hold all the electronics and work as a conceptual cane in this early prototype. This choice is due to the electromagnetic shielding that the conducting tube provides, to the physical robustness of such a tube, and because it is cheap, widely available and it is still a rough approximation of a blind's cane, making it a good compromise for a prototype.

As the diameter of the tube is only 2.5cm, it was not an easy task to fit all the desired circuits inside the tube. The design of the printed circuit board is presented in Figure 7-4 of page 99.

The PCB was positioned at the inside top of the tube, and the touch sensor electrode was placed in the topmost area of the PCB, perpendicular to it, so that when paired with its dielectric it also works as a cap of the tube. The vibration motor was also placed in the PCB. As the PCB was designed to fit snugly inside the tube, vibrations flow very well up to the hand of the user.

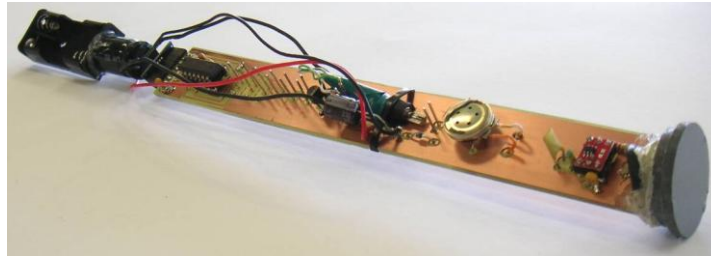


**Figure 4-10: PCB with relevant components of module #2**

The biggest advantages of the selected solar panel are, without doubt, its flexibility, lightweight and being unbreakable. This enables to roll the panel around the surface of the tube, requiring no special attention and care from the user and increasing the angle in which it can receive solar light as well as the overall robustness of the system. This would not be possible if a regular “glass” solar panel was used. As it is only for prototype, test and demonstration purposes, the panel and the LEDs were not permanently fixed to the tube, so that they can be changed and reused if needed.

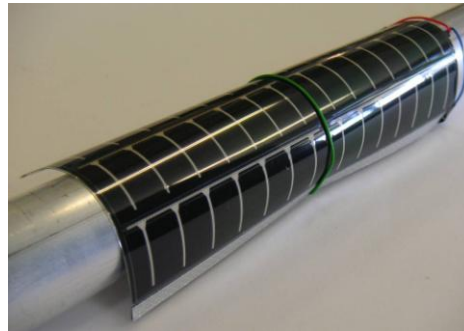


**Figure 4-11: Flexible solar panel placed around the prototype cane**

The LEDs were placed along each side of the cane. This makes it possible for the LEDs to be seen in almost every angle. All the wires coming from the LEDs as well as from the solar panel, travel inside the tube until they reach the top of the cane. There they are fitted with connectors that attach to the PCB.

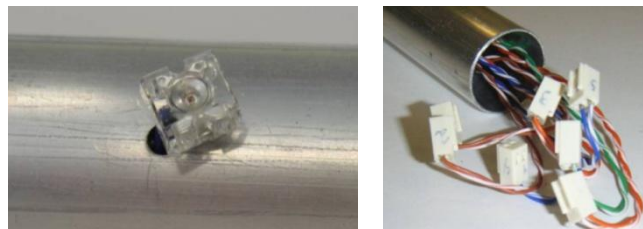


**Figure 4-12: High brightness LED and connectors**

The following pictures show the described prototype of module #2.



**Figure 4-13: Full prototype version of module #2**

### ***4.3.6 Results / Problems encountered***

During the development of this module several problems and difficulties appeared. The most complex of these problems concerns the software, specifically the low-power modes algorithms and the respective interrupts set by peripherals. Occasionally, it happened that when turning the cane off (actually putting it in a standby mode) using the touch sensor, the cane would not wake-up and turn on again. Only after thorough debug sessions, it was found that this problem was due to entering in low-power modes inside interrupt service routines, when the microcontroller was already in a low-power mode. Important to notice that in the Texas Instruments' MSP430 family, unlike what happens in most PICs from Microchip, each peripheral has its own independent interrupt service routine, making it harder to control when multiple interrupts occur at the same time or inside other ISRs. A great care had also to be taken not to lose the context of program execution, variables, etc, when using low-power modes. An example of this previous problem is when the CPU is waiting in a low-power mode for an ADC conversion and the user turns the cane off, generating an interrupt via the touch sensor. When waking-up again, the ADC would have to be initiated again, so the program would not be able to continue from the point where it stopped its execution. It was a hard task to prevent every possible occurrence of this problem to happen, but it was successfully achieved.

Another interesting problem found concerns the influence of electromagnetic fields in the environment around the electrode of the touch sensor. Sometimes, only by changing the position of the cane, the circuit would be unintentionally activated, like if someone had touched the touch sensor. To mitigate this problem, a great care was taken in shielding the areas near the electrode and its lines (also provided by the aluminium tube itself) to block possible noise and the sensitivity of the touch sensor was decreased. Nevertheless, the worst problem concerning the touch sensor is related to variations in the supply voltage. All the circuit was develop to work in a wide range of supple voltage, between 1.8V and 3.6V. Unfortunately, the supply voltage directly interferes with the touch sensor's sensibility: as higher the voltage, the most sensible the sensor becomes. When the changes in the supply voltage are slow, like when they are due to the normal draining of the batteries, they do not affect the circuit because the sensor auto-recalibrates itself from time to time.

The problem arises when there are sudden changes in the supply voltage, as for example when the batteries are low and the cane enters a high luminous intensity environment. When this occurs, the solar panel will supply 3.6V to the batteries in order to charge them, so the global voltage supplied to the circuit will suddenly increase. The touch sensor, which had previously calibrated itself for the lower voltage, will now increase its sensibility so much that it will unintentionally detect a false touch, turning the circuit off and not allowing it to be turned on again until the sensor auto-recalibrates (80 seconds) or until the solar panel stops receiving solar light. This situation is obviously unacceptable in an environment with constant changes in light intensity. Unfortunately, this behaviour was only detected when the prototype was already assembled, so a straightforward solution had to be found which could be implemented in the already developed and assembled circuit. The answer found to this problem consists in using a LED as a voltage regulator. This of course has the big disadvantage of greatly increasing the overall power consumption of the circuit, even when it is in the standby mode.

Figure 4-14 presents the regulation circuit.

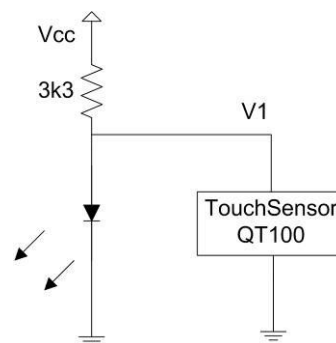


**Figure 4-14: Using an LED as a voltage regulator**

As can be easily seen in the picture, due to the LED polarization, the circuit is constantly consuming energy. Before the implementation of this regulator, the current consumption of the whole circuit in standby mode was around  $15\mu\text{A}$  (independent of voltage), increasing now this value to  $360\mu\text{A}@3\text{V}$  e  $188\mu\text{A}@2.4\text{V}$ . Although this represents indeed a significant increase in the consumption, it effectively improved the stability of the touch sensor's supply voltage (V1):

- For  $V_{cc}=2.1\text{V} \rightarrow V1=1.76\text{V}$
- For  $V_{cc}=3\text{V} \rightarrow V1=1.82\text{V}$

Concerning the solar panel, it was experimentally tested that the threshold voltage to detect darkness would be  $41\text{mV}$ . This value was enough to guarantee that the LEDs would not be activated in indoor environments with artificial light.

The voltage of the batteries was monitored and its value divided into five levels, making it possible to inform the user in a fast, clear and easy way about the charge level of the batteries.

- Level 1:  $V_{cc}$  (voltage of both batteries in series)  $< 2.2\text{V}$
- Level 2:  $2.2\text{V} \leq V_{cc} < 2.35\text{V}$
- Level 3:  $2.35\text{V} \leq V_{cc} < 2.5\text{V}$

- Level 4:  $2.5V \leq V_{cc} < 2.65V$
- Level 5:  $V_{cc} \geq 2.65V$

These levels correspond to the number of vibrations that the cane produces when indicating the voltage level of the batteries.

It was not easy to measure some specific current consumptions, especially the LEDs current and when the circuit is on. This is also due to the lack of appropriate measurement devices.

To measure the standby current (when the microcontroller is in a low-power mode and only the touch sensor remains active, although also in a low-power mode) a workbench ammeter was used in series with the supply line.

With the circuit turned on, but without blinking the LEDs and using the vibration motor, the supply current increases in average around  $80\mu A$ . When the LEDs are blinking, but still with the vibration motor inactive, the maximum current consumption of the circuit was around  $4mA$ . With the vibration motor active, the current increases to  $36mA$ , with a peak of  $40mA$  when the motor starts. It was found that when the solar panel is connected to the circuit without being exposed to solar light, the overall current consumption of the circuit increases about  $5\mu A$ .

### ***4.3.7 Conclusions***

The measured current consumption values are very encouraging and comply with the expected values, stated in the datasheets of the several components. According to these, the theoretical consumption in standby mode would be of  $0.1\mu A$  from the microcontroller, around  $12\mu A$  from the touch sensor and  $2\mu A$  from the buffers. The total value is, in fact, near the obtained value without the voltage regulator,  $15\mu A$ .

In the assembled version of module #2 prototype, it was realized that the sound of the speaker was not properly heard due to being closed inside the aluminium tube. This is undoubtedly one of the aspects to improve in future versions of this module, combined with the inclusion of a headphone jack to give one more option to user. Maybe it would be also reasonable also to include a wireless headset to provide audio signals if the user wishes so.

The LEDs proved to be effective and highly visible in dark conditions, improving thus the safety of the user.

Achieved vibration intensity proved to be enough for an accurate perception from the user.

## ***4.4 Proposed prototype of the cane – full system***

As said throughout the text, the two described modules that implement all the features of the cane were developed separately and independently. When both modules reached an advanced stage of development, a way to interconnect them had to be developed so that they could communicate and interact with each other. The initial objective for this stage was, due to the knowledge and experience gathered with the development of the modules, to design a completely new module that would incorporate improved versions of both presented modules. This new and more specific module would be smaller and lighter, use better components, have only one microcontroller, eliminate unnecessary circuits that were required during development, and gather all the circuits required to use and control the cane. Unfortunately, due to time restrictions, this was not possible,

and that is the reason why it was decided to use the already developed modules communicating with each other to fully control the cane. To do this, only some slight modifications had to be performed to interconnect the modules.

As the cane is purely a prototype to test the key concepts, there were also no concerns with the aesthetical side of the cane neither with the overall weight of the device.

In the next pictures, a diagram of the implemented connections is presented, followed by a photograph of the final prototype.

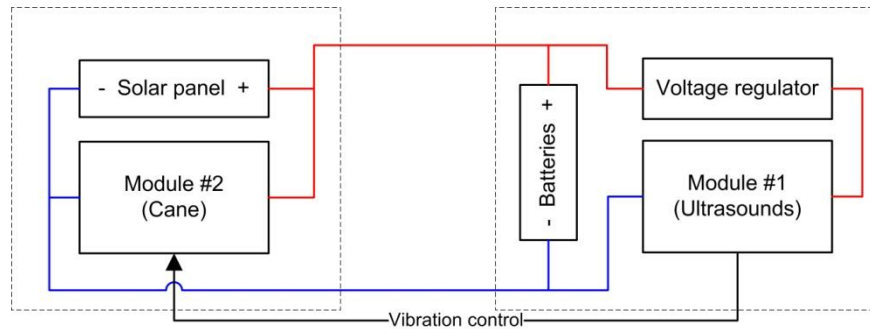


**Figure 4-15: Modules' interconnection diagram**

Module #1 analyses the floor and, whenever it detects a hole, step or drop-off, it sends a signal to module #2 that will cause an interrupt to alert the user via vibration and sound.

Module #2 is not physically turned OFF by the main ON/OFF switch of module#1. It detects the position of this button and automatically goes to sleep when module #1 is turned OFF, remaining in an ultra-low-power mode until module #1 is activated again. Even with the circuit turned OFF, the batteries are recharged by the solar panel, provided the panel is under direct sunlight.

Besides vibration and audible signals that alert the user in module #2, there are three LEDs in module #1 that provide information about the presence of a hole, drop-off or step, indicate when pulses of ultrasounds are being emitted, and show if the cane is ON or OFF.

A stripe of tape with a particular texture was placed along the side of the cane's handle that should face upwards, so that the user knows how to correctly hold the cane in order to guaranty that the ultrasonic sensors are correctly positioned, i.e., facing down, perpendicular to the ground.

All other aspects concerning the operation of the cane were maintained exactly as explained in each module's description.



**Figure 4-16: Prototype of the cane**

## 5 Field tests / Results

When the prototype was ready, it was imperative to test it with visually impaired persons, in real life situations. Only with genuine field tests it could be possible to evaluate the performance of the cane, its concepts and usability, as well as gather opinions, new ideas and possible improvements from the persons that will be using the cane. Only knowing the actual needs of visually impaired individuals and studying the way how they use such devices we can improved our device in order to make it truly useful.

Under this context, a meeting with blind persons from the APEC was scheduled so that field test could be conducted and opinions gathered.



**Figure 5-1: Field tests with a blind person**

Overall, the meeting and tests conducted were very successful. The users were very interested in the device and highly appreciated the functionalities and features provided by the cane. Although the tests were mostly conducted in Portuguese paving (the most problematic type of surface), the cane performed almost flawlessly, with very few false detections and accurately detecting significant holes, steps and drop-offs, like the end of sidewalks and stairs, indoors and outdoors.

It was very important to realise with more detail how a cane is actually used and that each blind person has a somewhat distinct way of using a cane. This will be important for future developments and improvements.

The conversations during the meeting were also very productive and allowed us to realize some features that can be introduced in the future to address a wider range of their needs. On the top of these needs resides the detection of obstacles at head level and obstacles that are placed above the level of the cane. This will be the next step of the cane's development.

Concerning, more specifically, the hole-detection task, they were very pleased with the results in every type of surfaces, although they suggested that smaller steps should also be detected (steps above 3 or 4 centimetres). Another aspect that needs to be improved is the response speed of the cane. At the present stage of development, there is a small delay between the instant when the sensors pass above a step and the instant when the motor vibrates. Although this delay is of only

some milliseconds, it can be too much for a fast walking person. Improvements must also be done concerning this issue.

An aspect that was especially focused by the visually impaired was the need to fold or split the cane in smaller parts, so that it can be easily carried when not in use and/or stored requiring less space.

Once again, it should be noted that aspects like the weight, size, design and ability to split were not taken into account in this first prototype stage. They will be addressed in future developments. In addition, it should be noted that parameters like the minimum detectable step can be easily changed and adjusted by changing thresholds in the software. Nonetheless, a decrease in the minimum detectable step will increase the number of false detections due to intense irregularities in the surfaces.

The test also proved the efficacy of the solar panel, that besides correctly detecting when to turn on the safety LEDs, also efficiently recharges the batteries, taking approximately 2 to 3 hours under direct sunlight to fully charge them. The safety LEDs also proved to be very effective and highly visible in dark environments, making it very unlikely for a driver not to see the cane during the night.

## 6 Conclusions

With the field tests conducted, it was clear that the concept of the hole-detecting cane was indeed valid and useful. The main goals were successfully achieved, and even the greatest difficulties concerning the use of ultrasounds in very irregular surfaces were effectively overcome. Thus, the objectives of this work were successfully accomplished.

Nonetheless, improvements can still be done. Some of the drawbacks described in the field tests would be solved simply by building the initially intended final version of the prototype that would gather both developed modules into only one circuit, with a single microcontroller, which would be placed inside the cane. This would end the need to use external wires and improve the weight and sturdiness of the cane, reducing the price, the number of components required and, consequently, the power consumption. It would also effectively improve the overall reaction speed of the cane when holes are detected, because no intermediate communications between independent circuits would be required.

As the cane is merely a prototype to test the desired key concepts, there were no concerns with the aesthetical side of the cane neither with the overall weight of the device. Nevertheless, this important issue will have to be taken into account for upcoming developments. Also having in mind future developments, some new ideas arise based on the tests conducted and on the feedback of the visually impaired. Among these is the addition of sensors to detect obstacles that cannot be detected by a traditional cane, especially obstacles at head height. A multi-sensor approach might also be developed to improve the detection of holes, drop-offs and steps. The purpose of these additional sensors would be to add redundancy to the system in order to improve the detection and reduce false detections. Light sensors, like infrared, can be used as well as more ultrasonic sensors.

Another interesting improvement would be to find a more power-efficient way to produce vibrations. This may be achieved by using piezoelectric transducers instead of the DC vibration motor (which is the component with the highest power consumption).

An encouraging achievement of this project was also the price of the hardware needed for the prototype, which is less than 80€.



## 7 Bibliography

- Pereira, Fábio (2005). *Microcontroladores MSP430: Teoria e Prática*. S.Paulo: Érica.
- Boico *et al.*: *Solar battery chargers for NiMH batteries*, IEEE Transactions on power electronics, Vol. 22, No. 5, September 2007.
- McClellan, J. H., Schafer, R. W. & Yoder, M. A. (2003). *Signal Processing First*. USA: Pearson Education.
- Chapman, S. J. (2004). *Matlab Programming for Engineers*. Canada: Thomson.
- “Ultrasound.” *Wikipedia, the free encyclopedia*. 02 Jun. 2008, <Reference.com <http://www.reference.com/browse/wiki/Ultrasound>>.
- “Ultrasound and Microcontroller Applications” *Hexamite*, 02 Jun. 2008, <http://www.hexamite.com/hetheory.htm>
- "Microcontroller." *Wikipedia, the free encyclopedia*. 02 Jun. 2008. <Reference.com <http://www.reference.com/browse/wiki/Microcontroller>>.
- "Multipath." *Wikipedia, the free encyclopedia*. 02 Jun. 2008. <Reference.com <http://www.reference.com/browse/wiki/Multipath>>.
- *Datasheet MSP430x20x2 and MSP430x22x4 mixed signal microcontrollers*, Texas Instruments.
- *MSP430x2xx Family User's Guide*, Texas Instruments.
- Datasheets of the several components used.



# Appendix A Circuit schematics

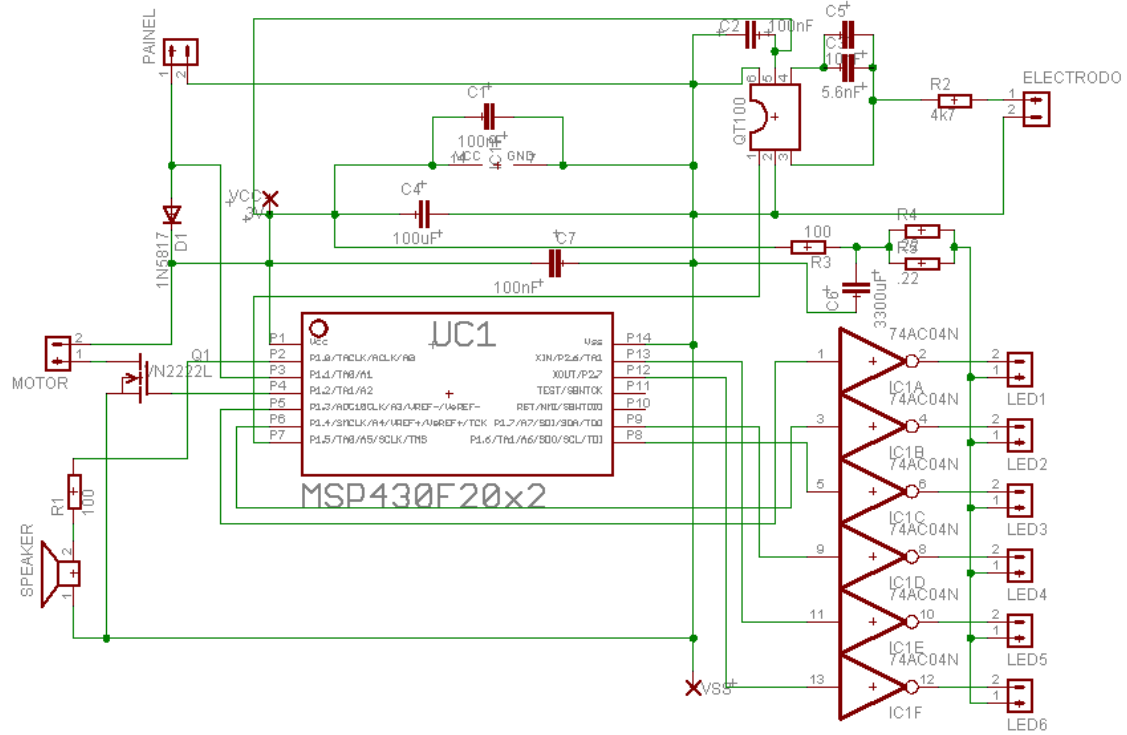
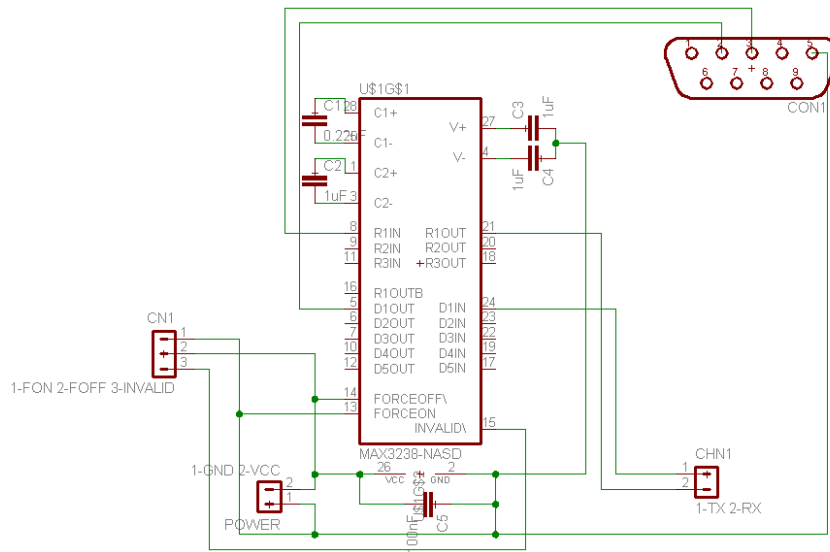


Figure 7-1: Electrical schematic of module #2





**Figure 7-3: Schematic of the external RS232 interface**



# Appendix B PCBs

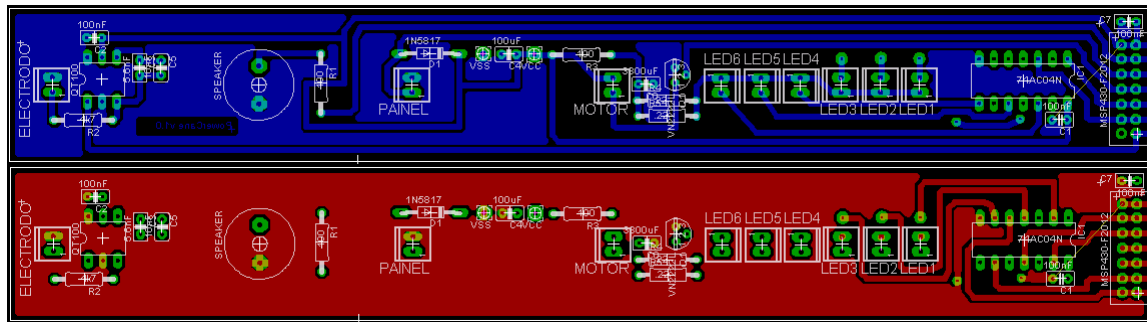


Figure 7-4: PCB of module #2 (bottom and top views)

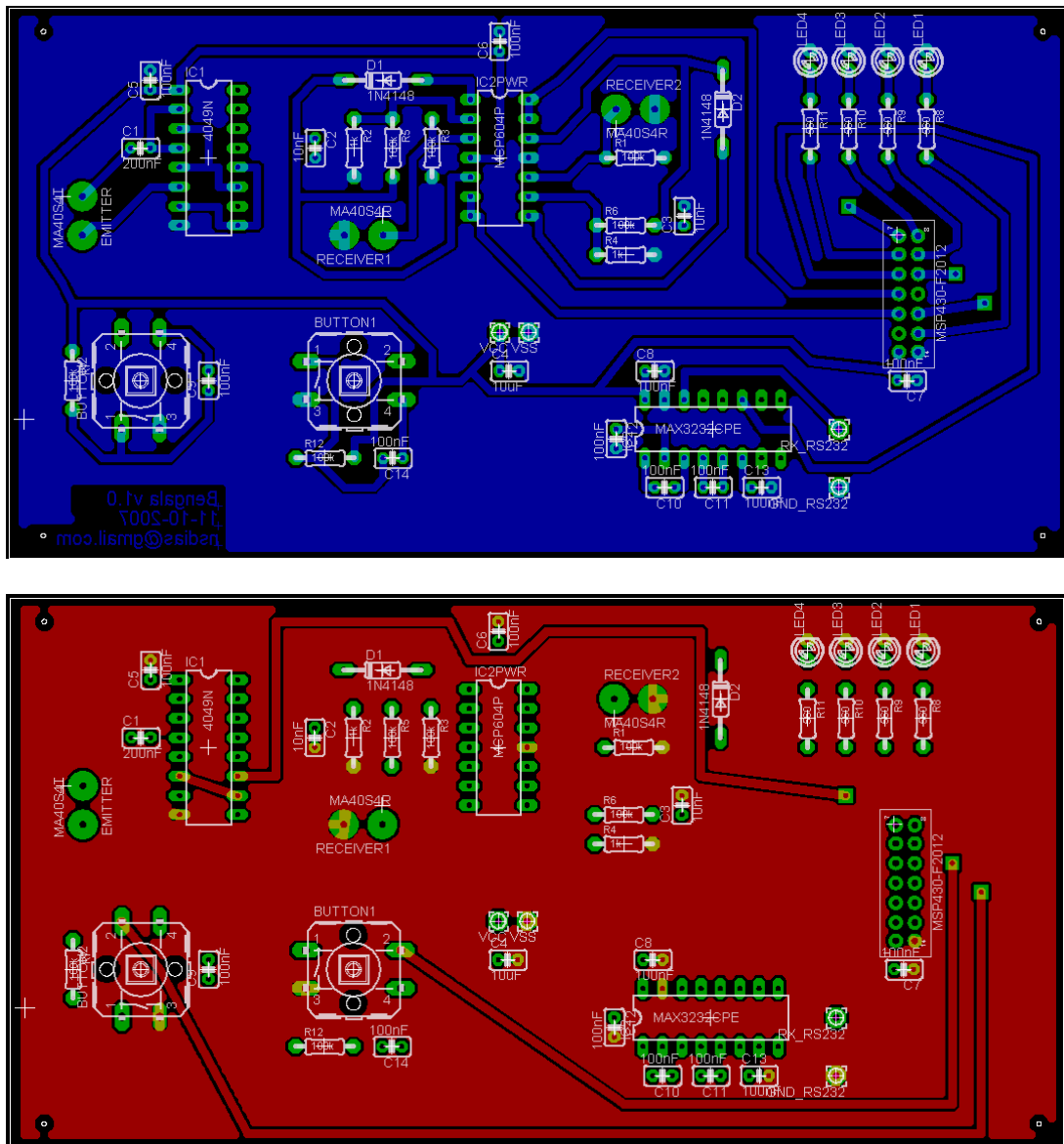


Figure 7-5: PCB of module #1 (bottom and top views)

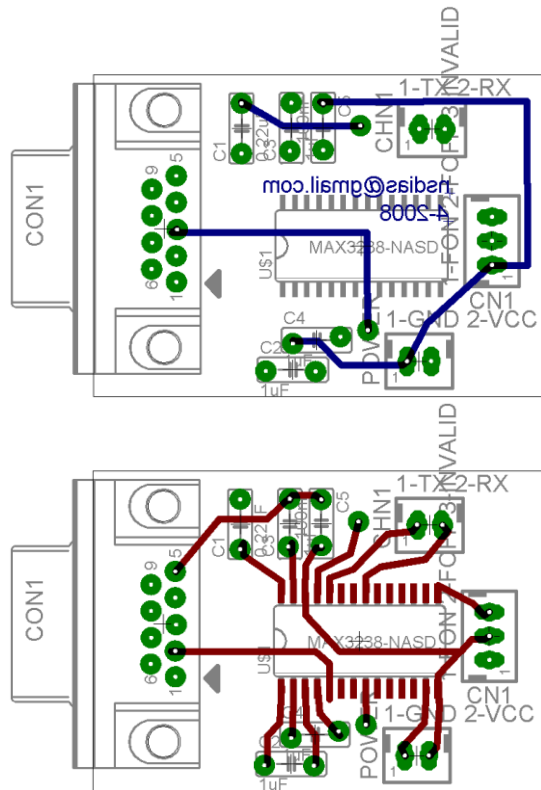


Figure 7-6: PCB of the external RS232 interface (bottom and top views)

## Appendix C Software

```
blink_top();
TACCR1=15000; // wait ~60ms
TACCTL1 &= ~CCIFG;
TACCTL1 |= CCIE; // Start the Timer
TACTL = TASSEL_2 + MC_2 + ID_2; // SMCLK, Continuous mode, prescaler=4, OVF interrupt disable
__bis_SR_register(LPM1_bits + GIE); // Enter LowPowerModel w/ interrupt enable

blink_middle();
TACCR1=15000; // wait ~60ms
TACCTL1 &= ~CCIFG;
TACCTL1 |= CCIE;
TACTL = TASSEL_2 + MC_2 + ID_2; // SMCLK, Continuous mode, prescaler=4, OVF interrupt disable
__bis_SR_register(LPM1_bits + GIE); // Enter LPM1 w/ interrupt

blink_bottom();
TACCR1=15000; // wait ~60ms
TACCTL1 &= ~CCIFG;
TACCTL1 |= CCIE;
TACTL = TASSEL_2 + MC_2 + ID_2; // SMCLK, Continuous mode, prescaler=4, OVF interrupt disable
__bis_SR_register(LPM1_bits + GIE); // Enter LPM1 w/ interrupt

blink_middle();
TACCR1=15000; // wait ~60ms
TACCTL1 &= ~CCIFG;
TACCTL1 |= CCIE;
TACTL = TASSEL_2 + MC_2 + ID_2; // SMCLK, Continuous mode, prescaler=4, OVF interrupt disable
__bis_SR_register(LPM1_bits + GIE); // Enter LPM1 w/ interrupt

blink_top();
```

Figure 7-7: Sequence for blinking the safety LEDs

```
/*
 * Routine for blinking the top LEDs
 */
// Each time this function is called, the top LEDs blink two time very fast.
// LED1 and LED4 blink alternately, each one at a time. They are never ON at the same time.
// This reduces possible supply current drops.
// The LEDs are not continually ON. They are driven with a PWM of about 37.3kHz, giving the
// feeling to the human eye that the LED is continually ON, with the same brightness,
// but in fact it is consuming almost half the current.
void blink_top(void)
{
    unsigned int g;

    LED1 = 1;
    for (g=800;g>0;g--) {LED1 ^= 1; LED4 ^= 1;}
    LED1 = 0; LED4 = 0;

    TACCR1=15000; // Wait ~120ms
    TACCTL1 &= ~CCIFG;
    TACCTL1 |= CCIE;
    TACTL = TASSEL_2 + MC_2 + ID_3; // SMCLK, Continuous mode, prescaler=8, OVF interrupt disable
    __bis_SR_register(LPM1_bits + GIE); // Enter LPM1 w/ interrupt

    LED1 = 1;
    for (g=800;g>0;g--) {LED1 ^= 1; LED4 ^= 1;}
    LED1 = 0; LED4 = 0;
}

```

Figure 7-8: Example of blinking a pair of LEDs

```

// ADC: Ref=2.5V; 16 clock cycles; 50ksps(low power); interrupt enable;
ADC10CTL0 = SREF_1 + ADC10SHT_2 + ADC10SR + REF2_5V + REFON + ADC10ON + ADC10IE;

//Waits 30us in LPM to allow Vref to settle
TACCR0 = 30; // Delay to allow Ref to settle (30us)
TACCTL0 &= ~CCIFG; // clear the interrupt flag
TACCTL0 |= CCIE; // Compare-mode interrupt enable
TACTL = TASSEL_2 | MC_1; // TACLK = SMCLK, Up mode
__bis_SR_register(LPM1_bits + GIE); // Enter LPM1 w/ interrupt

// Read the voltage of the solar panel
ADC10CTL1 = INCH_1; // ADC input A1
ADC10CTL0 |= ENC + ADC10SC; // Sampling and conversion start
__bis_SR_register(CPUOFF + GIE); // LPM0, ADC10_ISR will force exit

```

**Figure 7-9: Activation and use of the ADC to measure the voltage of the solar panel**

## Appendix D Characterization of the noise present in the received echoes

The code used throughout this section is presented in the file “sensors\_noise.m” (available in the CD-ROM attached).

$x$  is the number of the sample and  $y$  is the voltage of the signal where 40 corresponds to 58.7mV (the reference of the ADC is 1.5V which corresponds to 1023 in Matlab (10 bit ADC)).

### ❖ Test with the emitter turned on, sending pulses to a place without obstacles (thus in the presence of “crosstalk”)

- An average of 6661 readings was performed to obtain the following graphs.
- Files “R0a.mat” and “R1a.mat” include all the readings of each sensor (channel 0 and channel 1 respectively).

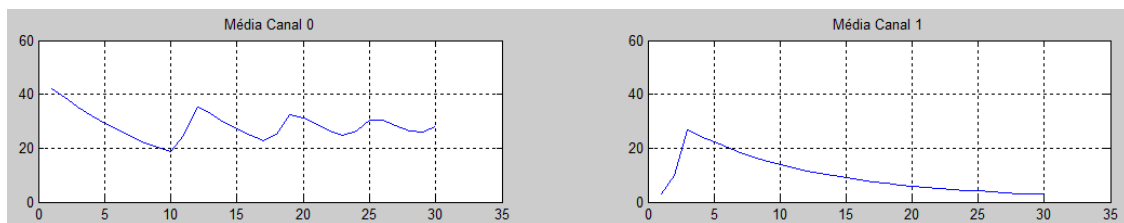


Figure 7-10: Average noise of channel 0 and channel 1 – emitter on

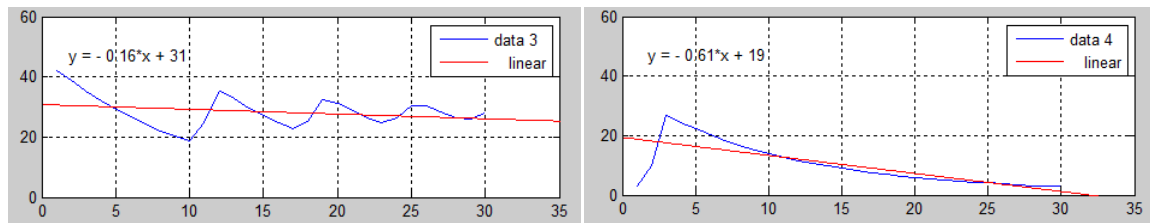


Figure 7-11: Linear fitting equations for channels 0 and 1 – emitter on

### ❖ Test with the emitter turned off (thus without any “crosstalk”)

- An average of 5179 readings was performed to obtain the following graphs.
- Files “R0b.mat” and “R1b.mat” include all the readings of each sensor (channel 0 and channel 1 respectively).

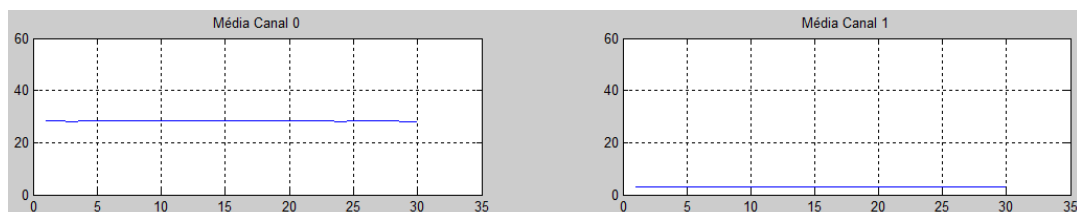


Figure 7-12: Average noise of channel 0 and channel 1 – emitter off

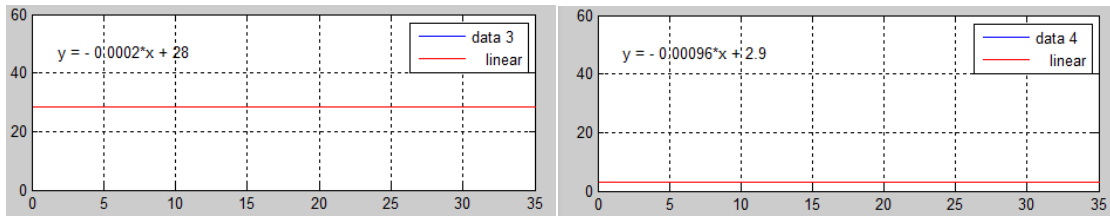


Figure 7-13: Linear fitting equations for channels 0 and 1 – emitter off

❖ Evaluation of the thresholds

- **Channel 0:**  $Threshold = -0.35x + 45$

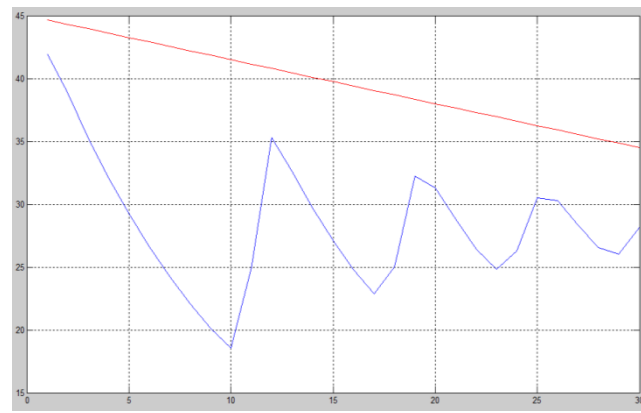


Figure 7-14: Calculated threshold for channel 0

- **Channel 1:**  $Threshold = -0.75x + 35$

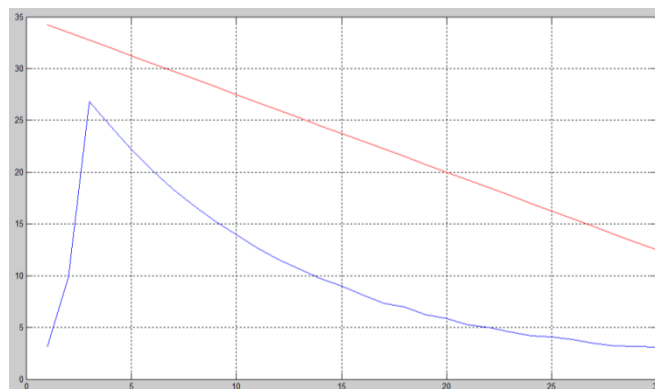
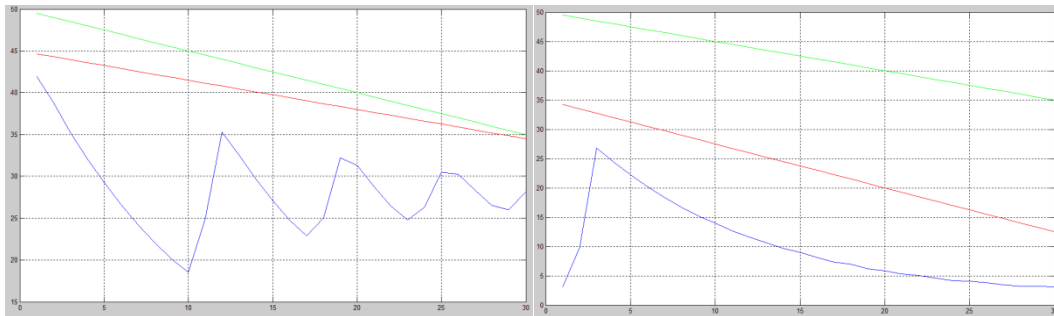


Figure 7-15: Calculated threshold for channel 1

❖ Threshold implementation for the microcontroller

A more straightforward way to implement these thresholds in the microcontroller is to use “ $-0.5x$ ” in the equations, because the division of a number by two only requires a binary shift to the right.

If we use the equation “ $Threshold = -0.5x + 50$ ” for both channels, the green line will be obtained.



**Figure 7-16: Thresholds comparison for channels 0 and 1**

As clearly shown in the previous graphs, these simpler thresholds are very close to the calculated ones requiring only an adjustment of the offset.

The final equations used are ( $x$  is the number of the sample):

- Channel 0:  $Threshold = 65 - \frac{x}{2}$
- Channel 1:  $Threshold = 50 - \frac{x}{2}$

Only values above this threshold will be considered.



## Appendix E Detection of sudden changes in the amplitude of the echoes

In the following graphs, each colour has represents a measure:

- **Blue:** maximum amplitude of the consecutive echoes.
- **Green:** derivative of the amplitude's variation, according to the following algorithm:

```
Nd2= 10;      % Order of the differentiator
h2= [-ones(1,Nd2/2) 0 0 ones(1,Nd2/2)];
for i=100:1:n_readings, % n_readings= 7666
    slope(i)= amplitude_max(i-(Nd2+1) : i)*h2';
end
```

- **Red:** Calculated distance (obtained using the already developed algorithm for distance measurement).

$x$  is the number of the sample and  $y$  is the voltage of the signal where the reference of the ADC is 1.5V which corresponds to 1023 in Matlab (10 bit ADC).

For the next graph, a set of pulses was acquired and stored in the following files (available in the CD-ROM attached):

- *Amplitude\_max.mat* – amplitudes of the echoes
- *Distancia.mat* – distance obtained by the already developed algorithm

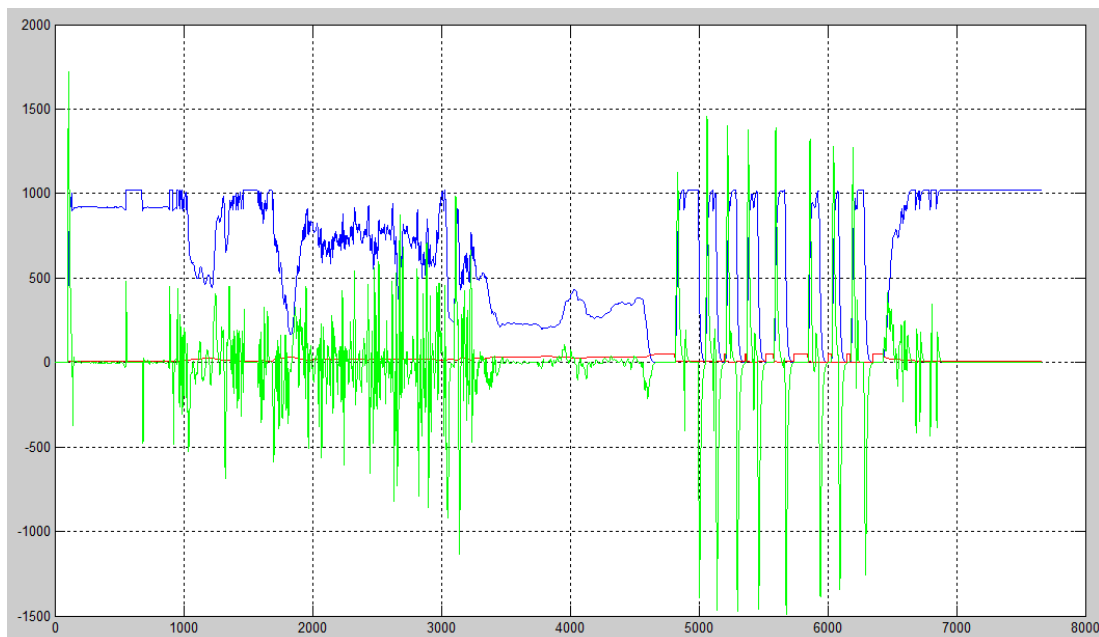
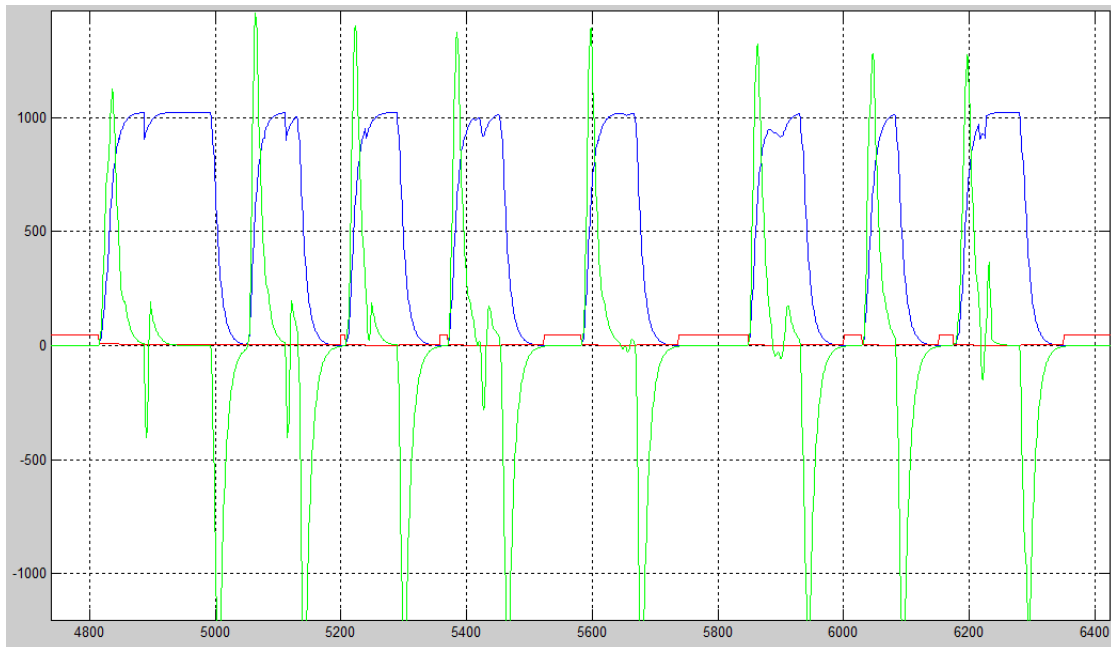


Figure 7-17: Example of the amplitude's slope detection algorithm

Now, a more specific test was conducted, moving the cane on the top of a high table (higher than the maximum detectable distance of 50cm) to the end of the table, where there would be no received echo. A continuous and repeated movement was performed with the sequence “table – no table – table – no table - ...” and so on, corresponding alternatively to received echoes and no received echoes. The results are showed in the next graph.



**Figure 7-18: Comparison between amplitude and distance detection algorithms when echoes stop being received during small instants**

As can be clearly seen in the graphs, in both situations but especially in cases where suddenly there are no echoes received, the amplitude detection algorithm performs a lot better than the distance algorithm. Abrupt changes in the amplitude of the received echoes (due to deep holes) are now detected flawlessly and almost instantly.

The reason why there is a considerable delay in the distance algorithm is that it must wait a certain amount of time until it detects the maximum distance due to the absence of an echo.

Just to give another example, a fast movement with the cane over a deep (more than 50cm) but narrow (around 10cm) hole, placed between two flat surfaces, was performed to evaluate the performance of this algorithm.

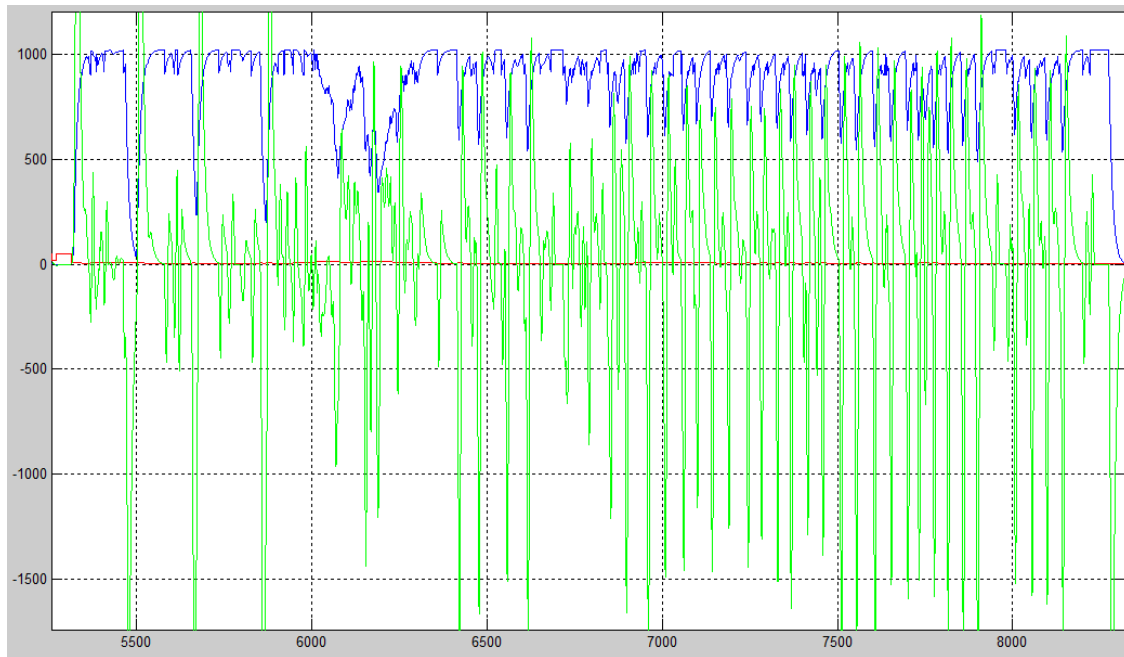


**Figure 7-19: Performance of both hole-detection algorithms over a deep and narrow hole**

The graph shows that although in the presence of a hole, the distance (in red) almost does not change, not detecting the hole. Nonetheless, the amplitude algorithm correctly detects the hole.

The main drawback of this algorithm is that in very irregular surfaces there are many sudden variations of the echoes' amplitude, which in turn may lead to false hole detections. Thus a great care must be taken in the decision of the threshold value. After thorough practical tests, the value 1800 proved to be a good compromise.